ФИЗИКА ЭЛЕМЕНТАРНЫХ ЧАСТИЦ И АТОМНОГО ЯДРА
2005. Т. 36. ВЫП. 3

УДК 539.12.01

FINITE MODELS OF THE OSCILLATOR

N. M. Atakishiyev[1,2], *G. S. Pogosyan*[1,3,4], *K. B. Wolf*[1]

[1]Centro de Ciencias Físicas, Universidad Nacional Autónoma de México, Cuernavaca, México
[2]Instituto de Matemáticas, Univesidad Nacional Autónoma de México, Cuernavaca, México
[3]Joint Institute for Nuclear Research, Dubna
[4]Departamento de Matemáticas, CUCEI-Ude G, AV. Corregiadora 500, Guadalajara, Jalisco, México

INTRODUCTION: WIGNER'S FREEDOM 473
THE OSCILLATOR GEOMETRIC AND DYNAMICAL POSTULATES 476
FINITE ONE-DIMENSIONAL OSCILLATOR 477
FINITE TWO-DIMENSIONAL OSCILLATOR 486
CONCLUSION: DISCRETE AND FINITE FOURIER TRANSFORMS 500

ФИЗИКА ЭЛЕМЕНТАРНЫХ ЧАСТИЦ И АТОМНОГО ЯДРА
2005. Т. 36. ВЫП. 3

УДК 539.12.01

FINITE MODELS OF THE OSCILLATOR

N. M. Atakishiyev[1,2], *G. S. Pogosyan*[1,3,4], *K. B. Wolf*[1]

[1]Centro de Ciencias Físicas, Universidad Nacional Autónoma de México, Cuernavaca, México
[2]Instituto de Matemáticas, Univesidad Nacional Autónoma de México, Cuernavaca, México
[3]Joint Institute for Nuclear Research, Dubna
[4]Departamento de Matemáticas, CUCEI-Ude G, AV. Corregiadora 500, Guadalajara, Jalisco, México

Finite oscillator models obey the same dynamics as the classical and quantum oscillators, but the operators corresponding to position, momentum, Hamiltonian, and angular momentum are generators of the compact Lie group $SO(D)$, and form the Lie algebra $so(D)$. One-dimensional finite oscillators, shallow planar optical waveguides, and finite data sets are $so(3)$ systems; and two-dimensional finite oscillators, shallow cylindrical waveguides, and pixellated screens are governed by $so(4)$. The physical reinterpretation of the generators of these algebras as observables that take a finite number of values, fits in a coherent picture of their phase space.

Модели конечного (финитного) осциллятора, обладающие той же динамикой, что и классический и квантовый осцилляторы, характеризуются тем, что операторы координаты, импульса, гамильтониана и углового момента в этих моделях являются генераторами компактной группы Ли $SO(D)$, образующими алгебру Ли $so(D)$. Одномерные финитные осцилляторы, плоские оптические волноводы и конечные наборы данных являются примерами $so(3)$-систем; двумерные финитные осцилляторы, плоские цилиндрические волноводы и пикселированные экраны описываются $so(4)$-системами. Физическая реинтерпретация генераторов этих алгебр как наблюдаемых, принимающих только конечное число значений, хорошо согласуется с когерентной структурой их фазового пространства.

1. INTRODUCTION: WIGNER'S FREEDOM

The question of whether or not the statement that the quantum mechanical operators obey the classical equations of motion, uniquely determines the quantization rule, $[\hat{q},\hat{p}] = i\hbar$, was posed by Wigner more than 50 years ago [1]. It was answered in the negative with a mild counterexample: A harmonic oscillator with the standard Hamiltonian $\hat{h}(p,q) = \frac{1}{2}(\hat{p}^2 + \hat{q}^2)$, that satisfies $[\hat{h},\hat{q}] = -i\hat{p}$ and $[\hat{h},\hat{p}] = i\hat{q}$, but with a displaced energy spectrum $E_n = E_0 + n\hbar$ ($n = 0, 1, \ldots$, and E_0 arbitrary), implies that the basic commutator will satisfy $([\hat{q},\hat{p}] - i\hbar)^2 = -(2E_0 - \hbar)^2$. We call this case *mild* because for $E_0 \neq \frac{1}{2}\hbar$, it amounts to little more than a change of scale in $\hbar$, although it opens the possibility that $[\hat{q},\hat{p}] - i\hbar$ be *any* operator whose square is unity.

Indeed, one has a larger — but well-defined — freedom in the choice of what the commutator between the position and momentum operators can be [2]. The realization that the quantum oscillator equations of motion are consistent with commutators other than $[\hat{q}, \hat{p}] = i\hbar$, came from optical image processing, in particular from the early applications of the fractional Fourier transform [3, Ch. X] to signal analysis on a finite number of discrete sensors or data points [4–6]. The physical model that realizes the simplest one-dimensional *finite oscillator*, is the shallow planar multimodal waveguide shown in Fig. 1: a light signal is a waveform $\psi(q)$, which is injected at the $z = 0$ line, and contains a distribution of space frequencies over this line, $\widetilde{\psi}(p)$. This waveform is then sensed at any

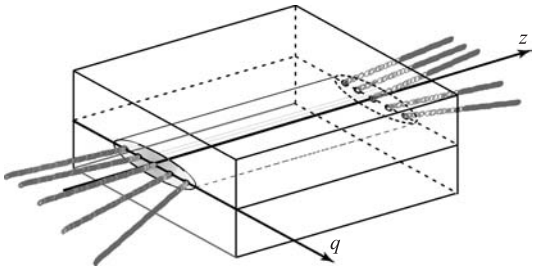

Fig. 1. The *finite oscillator* can be construed as a shallow, planar multimodal waveguide, which can carry only a finite number of modes (the rest are lost to the surrounding medium), and therefore cannot carry more information than that number of data values, at the same number of *sensor* points

other $z =$ constant «screen» line. (In paraxial optics, space frequencies are the momenta, and in the geometric picture they are related to the inclinations of rays.) Light travelling near to the axis z will evolve as a wavefunction in a quantum mechanical oscillator [7], with a Green function which is (a phase time) the fractional Fourier transform kernel [6]; but large space frequencies will leak out from the waveguide into the surrounding medium. There can be thus only a finite number of eigenmodes $\{\phi_n\}_{n=0}^{N}$ that the guide can propagate. And if only $N+1$ modes can exist in the guide, the transmitted signal itself cannot contain more than $N+1$ complex numbers; and not more than $N+1$ point-sensors are needed.

In Sec. 2 we introduce the postulates leading to the $(N+1)$-point finite oscillator model in D dimensions [5, 8, 9]. The finite model of the oscillator (or, for brevity, *finite oscillator*) by definition obeys the same dynamics as its classical, quantum and optical counterparts, but the operators of position $\mathbf{q}$, momentum $\mathbf{p}$ and the Hamiltonian h are made to close into the Lie algebra $so(D)$ of the *compact* Lie group $SO(D)$, rather than the traditional oscillator Lie algebra $\mathrm{osc}_D = \mathrm{span}\,(\mathbf{q}, \mathbf{p}, \hat{h}, \hat{1}\,)$, which is noncompact. The spectra and eigenfunctions of all operators in our model will be therefore necessarily finite in number.

In Sec. 3 we detail the one-dimensional case. There will be a ground state of the least energy, as well as a state of the highest energy, beyond which a shallow optical waveguide does not transmit. We essentially use a realization for the generators of the algebra $so(D)$ in terms of the *difference operators*. Then, raising and lowering operators within the algebra $so(D)$ provide a discrete Schrödinger *difference* equation, and the wavefunctions turn out to be the *Kravchuk functions*, long known as the small-d Wigner functions for $su(2)$. Although the difference equation does not manifestly separate into kinetic and potential energy summands, one can define an *equivalent* potential in terms of the finite oscillator ground state. Questions of analyticity of the solutions are addressed to give discrete systems a continuum aspect as well [4]. Lastly, we verify that the contraction limit $N \to \infty$ of the finite oscillator, when the interval and density of sensor points increases without limit, returns us to the ordinary quantum harmonic oscillator model.

In dimension $D = 1$, with the 3 operators q, p, h, there is but a single choice for the Lie dynamical algebra describing a finite linear oscillator, planar waveguide, or finite data set. For the case of dimension $D = 2$, in Sec. 4 we examine the oscillator model which is built as the direct product of two one-dimensional oscillators along Cartesian axes x and y. The algebra has then 6 generators that close into $su(2)^{(x)} \oplus su(2)^{(y)} = so(4)$, and describes a finite plane oscillator, a cylindrical waveguide, or a screen pixellated in Cartesian coordinates, with $(N+1)^2$ data points. Working with two-dimensional models we must expect further nonstandard commutators between position and momentum operators. Indeed, this can happen in more than one way when different subalgebra chains exist, i.e., when the original system yields to separation of variables in distinct coordinate systems [10]. We use the chains $so(2) \oplus so(2) \subset so(4) \supset so(3) \supset so(2)$, to describe the finite two-dimensional oscillator in polar coordinates, which is a discrete version for separation of variables with $(N+1)^2$ points [8, 9]. The finite radial wavefunctions turn out to be the Clebsch–Gordan coefficients — *Hahn functions*, and their recursion relations provide their finite radial Schrödinger equations. The equivalent potential of the radial oscillator presents a centrifugal barrier aspect. At the end of the section we again verify that when $N \to \infty$, and the interval and density of points grow jointly, in the contraction limit one recovers the ordinary quantum system with its Lie algebra, radial Schrödinger differential equation and wavefunctions.

These developments are aimed at elucidating the nature of phase space in finite Hamiltonian systems. In the concluding Sec. 5, we broach the question of fractional Fourier transformation of discrete, finite data sets which, as Fig. 1 suggests, are a string of data points between 0 and N, which are at the extremes of the set — and *not* periodic signals, as the traditional finite Fourier transform that engineering practitioners generally assume [11–14]. This Section adds some

considerations on the phase space of discrete, finite Hamiltonian systems, based on work which builds corresponding Wigner functions over *sui generis* phase spaces [15, 49].

In this paper we hope to show some of the definite advantages in proposing *precontracted* compact, finite models to quantum mechanics and wave optics, and unitary transformations of pixellated images, within a Lie-theoretic framework, because of the wealth of emerging results.

2. THE OSCILLATOR GEOMETRIC AND DYNAMICAL POSTULATES

The time evolution of a classical particle in a harmonic oscillator potential $\frac{1}{2}\omega|\mathbf{q}|^2$ is given by its Newton equation, or equivalently, its two Hamilton equations (using Poisson brackets)

$$\ddot{\mathbf{q}} = -\omega^2\mathbf{q} \Leftrightarrow \begin{cases} \{h, \mathbf{q}\} = -\mathbf{p}, \\ \{h, \mathbf{p}\} = \quad \mathbf{q}, \end{cases} \tag{1}$$

with the Hamiltonian function $h = \frac{1}{2}(\mathbf{p}^2 + \omega^2\mathbf{q}^2)$. The first Hamilton equation is geometric (it defines the momentum vector as tangent to the trajectory), while the second embodies the dynamics of the oscillator system. At little extra cost we can work in D dimensions, where the second-rank skew-symmetric tensor of angular momentum is $\widehat{m} = \mathbf{q}\times\mathbf{p}$. Since the Poisson bracket defines a derivation, it follows that $\{h, \widehat{m}\} = 0$, so the components of angular momentum are conserved. They generate joint rotations of $\mathbf{q}$ space and $\mathbf{p}$ space, namely

$$\begin{array}{c} m_{j,k} = q_j p_k - q_k p_j \\ j, k = 1, 2, \ldots, D \end{array} \quad \begin{cases} \{m_{j,k}, q_\ell\} = \delta_{j,\ell} q_k - \delta_{k,\ell} q_j, \\ \{m_{j,k}, p_\ell\} = \delta_{j,\ell} p_k - \delta_{k,\ell} p_j. \end{cases} \tag{2}$$

And finally, the components of angular momentum close under Poisson brackets into the Lie algebra $so(D)$ of rotations, which we specify below.

Schrödinger quantization replaces Poisson brackets of quadratic functions of phase space, by commutators of operators in a Hilbert space (indicated by capital letters), times $-i$. For the harmonic oscillator, the resulting quantum Newton and Hamilton equations are

$$[H, [H, \mathbf{Q}]] = \omega^2\mathbf{Q} \Leftrightarrow \begin{cases} [H, \mathbf{Q}] = -i\mathbf{P}, \\ [H, \mathbf{P}] = \quad i\mathbf{Q}. \end{cases} \tag{3}$$

The two Hamilton equations again display the separation between geometry and dynamics in oscillator systems. The Schrödinger quantization of $\widehat{m}$ correctly

produces the quantum angular momentum tensor operator, with Lie brackets

$$[H, M_{j,k}] = 0, \qquad \begin{aligned} [M_{j,k}, Q_\ell] &= i(\delta_{j,\ell} Q_k - \delta_{k,\ell} Q_j), \\ [M_{j,k}, P_\ell] &= i(\delta_{j,\ell} P_k - \delta_{k,\ell} P_j). \end{aligned} \tag{4}$$

Between these $\frac{1}{2}D(D+1)$ components of angular momentum, the commutators of the operators $M_{j,k} = -M_{k,j}$ are

$$[M_{j,k}, M_{\ell,n}] = i(\delta_{j,\ell} M_{k,n} + \delta_{k,n} M_{j,\ell} + \delta_{n,j} M_{\ell,k} + \delta_{\ell,k} M_{n,j}), \tag{5}$$

and this defines the Lie algebra $so(D)$, — independently of the realization of the generators.

Now we observe that the commutators $[Q_j, P_k]$ are thus far unspecified, and herein lies our choice:

If we require that the operators, Q_j, P_k, $M_{l,m}$ and H — and also the unity operator $\hat{1}$ — close into an *associative algebra*, then they must satisfy the Jacobi identity,

$$[X, [Y, Z]] + [Y, [Z, X]] + [Z, [X, Y]] = 0. \tag{6}$$

In view of Eqs. (3), the Jacobi identity for $X = H$ and $\{Y, Z\} = \{Q_j, P_k\}$, requires that

$$[H, [Q_j, Q_k]] = 0, \quad [H, [P_j, P_k]] = 0, \quad [H, [Q_j, P_k]] = 0. \tag{7}$$

These heretofore unspecified commutators, $[Q_j, Q_k]$, $[P_j, P_k]$, and $[Q_j, P_k]$, consistently close into the same algebra when we choose

$$[Q_j, Q_k] = iM_{j,k}, \quad [P_j, P_k] = iM_{j,k}, \quad [Q_j, P_k] = i\delta_{j,k} f(H, C), \tag{8}$$

where f is a linear function of the Hamiltonian H and Casimir operator C of the resulting algebra. The Jacobi identity is rather restrictive; it does not allow us, for example, to add a term $\sim M_{j,k}$ to the last commutator in (8), nor to consider nonlinear functions $f(H)$ when $D > 1$. Additional comments for a nonlinear function f in the case $D = 1$ will be presented in the concluding Section.

3. FINITE ONE-DIMENSIONAL OSCILLATOR

In the one-dimensional finite oscillator model there is a single position operator Q, its corresponding momentum P, and the Hamiltonian H. Their eigenvalues will be the observables of position, momentum, and energy, respectively.

3.1. The Finite Oscillator Dynamical Algebra $u(2)$. The Lie algebra into which we shall fit the finite oscillator dynamical observables will be $so(3) = su(2)$. Its generators are commonly associated to quantum angular momentum and realized as

$$J_j := -i\left(x_k\frac{\partial}{\partial x_l} - x_l\frac{\partial}{\partial x_k}\right), \quad j,k,l \text{ cyclic permutations of } 1,2,3, \tag{9}$$

on the space $\mathcal{A}_3$ of analytic functions of $\{x_k\} \in \Re^3$; they present the Lie brackets

$$[J_j, J_k] = iJ_l, \qquad j,k,l \text{ cyclic permutations of } 1,2,3. \tag{10}$$

There is a fourth, central «number» operator

$$E_J := \sum_{k=1}^{3} x_k\frac{\partial}{\partial x_k}, \qquad [E_J, J_k] = 0, \tag{11}$$

whose eigenvalues in $\mathcal{A}_3$ are $j \in \{0,1,2,\ldots\}$, which separate this space into finite-dimensional irreducible representations of $so(3)$, of dimensions $2j+1$. This completes the algebra to $u(1) \oplus su(2) = u(2)$, and binds the Casimir operator of $su(2)$ to be

$$C := |\mathbf{J}|^2 = \sum_{k=1}^{3} J_k^2 = E_J(E_J+1), \tag{12}$$

with eigenvalues $j(j+1)$ on the space of harmonic functions on the sphere. In every $\Re^{2j+1}$, the spectrum of each $su(2)$ generator J_k is

$$m \in \{-j, -j+1, \ldots, j\}. \tag{13}$$

Half-integer values $j \in \left\{\frac{1}{2}, \frac{3}{2}, \frac{5}{2}, \ldots\right\}$ occur in spin spaces that we can handle abstractly.

We now introduce [4–6] a new physical interpretation for the generators of $su(2)$ and their eigenvalues, to satisfy the postulates (3) of the harmonic oscillator on every finite-dimensional irreducible representation space $\Re^{2j+1}$ labelled by $j = \frac{1}{2}N$:

$$Q = J_1 \quad \longleftrightarrow \quad \text{position} \qquad q \in \{-j, -j+1, \ldots, j\}, \tag{14}$$

$$-P = J_2 \quad \longleftrightarrow \quad -\text{momentum} \qquad p \in \{-j, -j+1, \ldots, j\}, \tag{15}$$

$$H = J_3 + j + \frac{1}{2} \quad \longleftrightarrow \quad \text{Hamiltonian} \qquad h \in \left\{\frac{1}{2}, \frac{3}{2}, \ldots, 2j+\frac{1}{2}\right\}, \tag{16}$$

where

$$H - \frac{1}{2} = J_3 + j \text{ is the mode number} \qquad n \in \{0, 1, \ldots, N\},\ N := 2j. \quad (17)$$

These asignments fit in a diagram [17] where the generators for $su(2) = so(3)$, $\Lambda_{j,k}$, $1 \leqslant j < k \leqslant 3$, are placed in the j–k box as follows:

$$\begin{array}{|c|c|}\hline \Lambda_{1,2} & \Lambda_{1,3} \\ \hline & \Lambda_{2,3} \\ \hline \end{array} \quad = \quad \begin{array}{|c|c|}\hline J_3 & -J_2 \\ \hline & J_1 \\ \hline \end{array} \quad = \quad \begin{array}{|c|c|}\hline H-j-1/2 & P \\ \hline & Q \\ \hline \end{array} \qquad (18)$$

The basic commutator between position and momentum in the finite oscillator model on $\Re^{2j+1}$ is thus

$$[Q, P] = i\left(H - E_J - \frac{1}{2}\hat{1}\right) = iH - i\left(j + \frac{1}{2}\right)\hat{1}, \qquad (19)$$

and this system will have therefore intrinsically *discrete and finite* positions and momenta.

3.2. Position and Mode Eigenbases. Within the $su(2)$ representation $j = \frac{1}{2}N$, the finite oscillator consists of $N+1$ equidistant points $\left\{-\frac{1}{2}N, -\frac{1}{2}N + 1, \ldots, \frac{1}{2}N\right\}$, there are $N+1$ Kronecker eigenstates of $Q = J_1$. We use the familiar labeled-ket notation to characterize them by

$$\begin{aligned} Q\,|N, q\rangle_1 &= q\,|N, q\rangle_1, \qquad\qquad q|_{-N/2}^{N/2}, \\ \mathbf{J}^2\,|N, q\rangle_1 &= \frac{1}{2}N\left(\frac{1}{2}N + 1\right)|N, q\rangle_1. \end{aligned} \qquad (20)$$

A finite oscillator of $N+1$ points has also $N+1$ energy eigenstates of the Hamiltonian $H = J_3$, which has a ground state and the *highest* state in the system. This is the second eigenbasis:

$$\begin{aligned} H\,|N, n\rangle_H &= \left(n + \frac{1}{2}\right)|N, n\rangle_H, \qquad n|_0^N, \\ \mathbf{J}^2\,|N, n\rangle_H &= \frac{1}{2}N\left(\frac{1}{2}N + 1\right)|N, n\rangle_H. \end{aligned} \qquad (21)$$

Mode number $n|_0^N$ is related to the J_3 eigenvalues $\mu|_{-j}^{j}$, through $n = j + \mu$ and $\mu = n - \frac{1}{2}N$.

It is useful to denote the abstract $su(2) \supset u(1)_1$ and $su(2) \supset u(1)_3$ kets with round brackets:

$$\begin{array}{rclcrcl} |j,\mu)_3 & := & |2j, j+\mu\rangle_H, & & J_3\,|j,\mu)_3 & = & \mu\,|j,\mu)_3, \quad \mu|_{-j}^{j}, \\ |N,n\rangle_H & := & \left|\frac{1}{2}N, n-j\right)_3, & & \mathbf{J}^2\,|j,\mu)_3 & = & j(j+1)\,|j,\mu)_3. \end{array} \tag{22}$$

They are related by a rotation to each other, through

$$\mathrm{e}^{-i\frac{1}{2}\pi J_2}\,J_3 = J_1\,\mathrm{e}^{-i\frac{1}{2}\pi J_2} \quad \Rightarrow \quad |N,q\rangle_1 = \mathrm{e}^{-i\frac{1}{2}\pi J_2}\;|N, j+q\rangle_H. \tag{23}$$

Their *overlap* is thus a «small-d» Wigner function [18],

$$d^j_{m,m'}(\beta) \;:=\; {}_3(j,m|\,\mathrm{e}^{-i\beta J_2}\,|j,m')_3 = d^j_{m',m}(-\beta) = \tag{24}$$

$$= \sqrt{(j+m)!\,(j-m)!\,(j+m')!\,(j-m')!}\,\times$$

$$\times \sum_k (-1)^k \frac{\left(\cos\frac{1}{2}\beta\right)^{2j-2k+m-m'} \left(\sin\frac{1}{2}\beta\right)^{2k-m+m'}}{k!\,(j+m-k)!\,(j-m'-k)!\,(m'-m+k)!}. \tag{25}$$

3.3. Kravchuk Functions of the Finite Oscillator. The wavefunctions of the finite oscillator are the overlaps between the position Q-basis and the energy H-basis vectors. From (22), (23), and (24), they are

$$\Phi_n^{(N)}(q) \;:=\; {}_1\langle N,q|N,n\rangle_H = {}_H\langle N, j+q|\,\mathrm{e}^{+i\frac{\pi}{2}J_2}\,|N,n\rangle_H = \tag{26}$$

$$= d^j_{q,n-j}\left(-\frac{1}{2}\pi\right) = d^j_{n-j,q}\left(\frac{1}{2}\pi\right) = \tag{27}$$

$$= \frac{(-1)^n}{2^j}\sqrt{\binom{2j}{n}\binom{2j}{j+q}}\,K_n\left(j{+}q; \frac{1}{2}, 2j\right) \tag{28}$$

for $N = 2j,\ n|_0^N,\ q|_{-j}^j$. The last line is the explicit expression, which is written with the square root of two binomial distributions and a *symmetric Kravchuk polynomial* [19] in $j{+}q$:

$$K_n\left(x; \frac{1}{2}, N\right) := {}_2F_1(-n, -x; -N; 2). \tag{29}$$

We observe the self-duality of the Kravchuk polynomials, namely

$$K_n\left(x; \frac{1}{2}, N\right) = K_x\left(n; \frac{1}{2}, N\right), \tag{30}$$

when both x and n are integers in the interval $[0, N]$.

The finite oscillator wavefunctions $\Phi_n^{(N)}(q)$ in (28) are thus called *Kravchuk functions*. These wavefunctions satisfy *no* differential equation, but a Schrödinger *difference* equation (see (33) below), which relates the values of the functions on three not necessarily integer points, separated by one unit [20]. From the difference equation for Kravchuk polynomials [21], which follows from the familiar raising and lowering relations between $su(2)$ states, results the Schrödinger difference operator

$$H^j(q) = -\frac{1}{2}[\alpha^j(q)\,\mathrm{e}^{-\partial_q} - (2j+1) + \alpha^j(-q)\,\mathrm{e}^{+\partial_q}], \quad (31)$$

$$\alpha^j(q) := \sqrt{(j+q+1)(j-q)} = \alpha^j(-q-1), \quad (32)$$

$$H^j(q)\,\Phi_n^{(N)}(q) = E_n\,\Phi_n^{(N)}(q), \text{ where } E_n = n + \frac{1}{2},\ n|_0^N. \quad (33)$$

The (real) discrete orthogonality and completeness relations satisfied by the $N+1$ finite oscillator states are

$$\sum_{q=-j}^{j=\frac{1}{2}N} \Phi_n^{(N)}(q)\Phi_{n'}^{(N)}(q) = \delta_{n,n'}, \quad \sum_{n=0}^{N=2j} \Phi_n^{(N)}(q)\Phi_n^{(N)}(q') = \delta_{q,q'}. \quad (34)$$

In Fig. 2 we show the bottom, middle and top wavefunctions of the finite oscillator.

3.4. Finite Oscillator Equivalent Potential. We should note that the difference Hamiltonian (31) does not separate into a sum of a kinetic plus potential energy terms. However, one can introduce [22] a discrete *equivalent* potential, based on the continuous model of a system with a potential $V(q)$ and energy $E_0 > -\infty$, whose ground state $\Psi_0(q)$ has no zeros and determines the potential energy from the Schrödinger equation:

$$\left(-\frac{1}{2}\frac{d^2}{dq^2} + V(q) - E_0\right)\Psi_0(q) = 0 \Rightarrow V(q) - E_0 = \frac{1}{2}\frac{d^2}{dq^2}\Psi_0(q)\Big/\Psi_0(q). \quad (35)$$

In the case of the harmonic oscillator, $\Psi_0(q) \sim \mathrm{e}^{-\frac{1}{2}q^2}$, so that $\dfrac{d^2}{dq^2}\Psi_0(q) = (q^2-1)\Psi_0(q)$, and (35) yields correctly $V(q) - E_0 = \dfrac{1}{2}q^2 - \dfrac{1}{2}$.

In the discrete case of the equidistant points $q \in \{-j, -j+1, \ldots, j\}$, the ground state of the eigenfunction set (26)–(28) is

$$\Phi_0^{(N)}(q) = d^j_{-j,q}\left(\frac{1}{2}\pi\right) = \frac{1}{2^j}\sqrt{\frac{(2j)!}{(j+q)!\,(j-q)!}}, \quad (36)$$

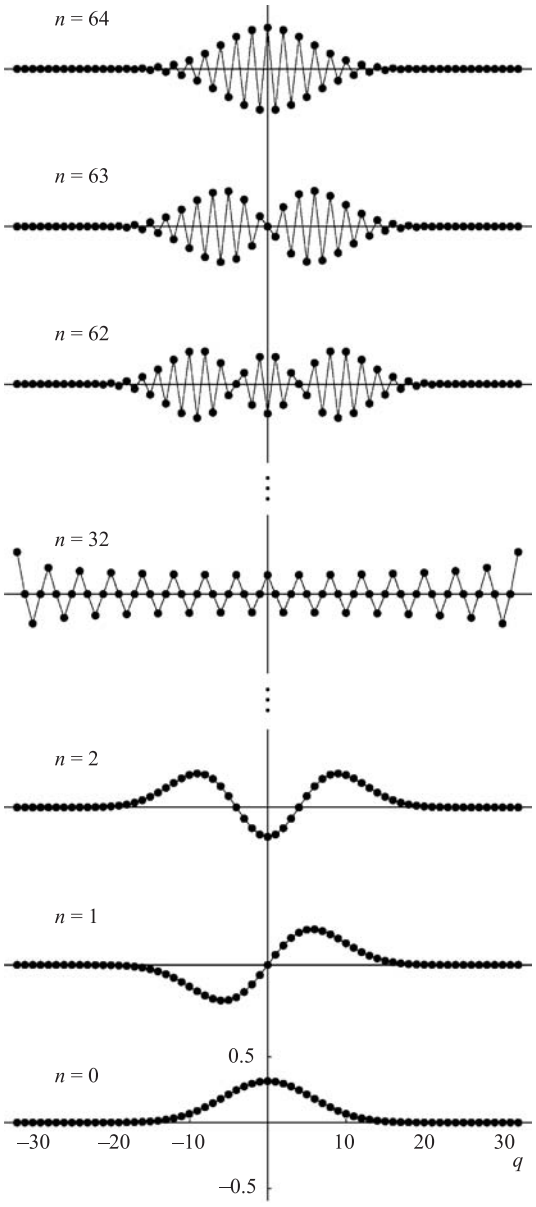

Fig. 2. The finite oscillator Kravchuk wavefunctions for $j = 32$, so there are $2j + 1 = 65$ points along the q axis (joined by straight lines for visibility) for $n = 0, 1, 2, \ldots, 32, \ldots, 62, 63, 64$, from bottom to top

since $K_0(x;p,2j) = 1$. The second difference operator yields explicitly the following equivalent potential $V(q)$:

$$V(q) - E_0 + 1 = \frac{\Phi_0^{(N)}(q+1) + \Phi_0^{(N)}(q-1)}{2\Phi_0^{(N)}(q)} = \tag{37}$$

$$= \frac{\sqrt{(j+q)(j+q+1)} + \sqrt{(j-q)(j-q+1)}}{2\sqrt{(j+1)^2 - q^2}}, \tag{38}$$

which is shown in Fig. 3 for various values of $N = 2j$. In the finite oscillator, the ground state $\Phi_0^{(N)}(q)$ can be analytically continued in q everywhere in the complex plane, except for branch-point zeros at $q = \pm(j+1)$, which are due to the square root of the binomial distribution. The wavefunctions themselves are thus well defined and «continuous» for any real value of q within the interval $-(j+1) \leqslant q \leqslant j+1$, which is one unit beyond their natural orthogonality endpoints in (34).

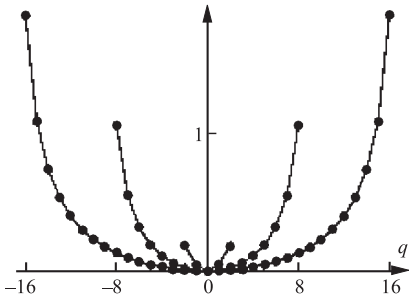

Fig. 3. The finite oscillator equivalent potential for $j = 2$, 8, 16 (i.e., for 5, 17 and 33 points). We have added $\sqrt{j/(j+1)}$ so that all potentials coincide for the centre point $q = 0$

3.5. Contraction of the Algebra $u(2) \to \mathrm{osc}$. The finite oscillator model described in the previous Section, contracts to the standard quantum harmonic oscillator, on the level of the algebra, the Schrödinger equation, and the solution wavefunctions [23]. While the three generators of $su(2)$ in $u(2)$ are equivalent, since they can be rotated one onto the other, the contraction process breaks this symmetry to distinguish one axis — that of the Hamiltonian — which retains its discrete spectrum, from the other two axes of position and momentum, whose spectrum «becomes» continuous. The quotes indicate the usual distinction between a sequence of Hilbert spaces of increasing finite dimension and its limit, the space of Lebesgue square-integrable functions on the real line.

The Wigner–Talman [24] contraction of $su(2)$ representations of increasing dimension $2j+1$ as $j \to \infty$ to the representations of the Heisenberg–Weyl algebra $\mathrm{HW}_1 = \mathrm{span}\,\{\hat{Q}, \hat{P}, \hat{1}\}$, for $\hbar = 1$, is well known (see, e.g., [25–27]). The present contraction of the finite oscillator is different [23]: as the number of points and interval increases as $j \to \infty$, and their spacing in position and momentum

decreases appropriately, all four generators of its dynamical algebra contract to the oscillator algebra,

$$\lim_{j\to\infty} u(2) \longrightarrow \mathrm{osc}_1 = \{\hat{H}, \hat{Q}, \hat{P}, \hat{1}\} \supset \mathrm{HW}_1 = \{\hat{Q}, \hat{P}, \hat{1}\}. \tag{39}$$

We introduce a new basis for the four generators of $u(2) = \mathrm{span}\,\{E_J, \mathbf{J}\}$ (see (14)–(17)), within the $(2j{+}1)$-dimensional representation j,

$$\begin{pmatrix} Q^{(j)} \\ P^{(j)} \\ H^{(j)} \\ \hat{1} \end{pmatrix} = \begin{pmatrix} j^{-1/2} & 0 & 0 & 0 \\ 0 & j^{-1/2} & 0 & 0 \\ 0 & 0 & 1 & 1+1/2j \\ 0 & 0 & 0 & j^{-1} \end{pmatrix} \begin{pmatrix} J_1 \\ J_2 \\ J_3 \\ E_J \end{pmatrix}, \tag{40}$$

whose nonzero commutators are then

$$[H^{(j)}, Q^{(j)}] = iP^{(j)},\ [H^{(j)}, P^{(j)}] = -iQ^{(j)},\ [Q^{(j)}, P^{(j)}] = i\hat{1}{+}ij^{-1}H^{(j)}. \tag{41}$$

As $j \to \infty$, these become those of H_4, namely

$$[H^{(\infty)}, Q^{(\infty)}] = iP^{(\infty)},\ [H^{(\infty)}, P^{(\infty)}] = -iQ^{(\infty)},\ [Q^{(\infty)}, P^{(\infty)}] = i\hat{1}, \tag{42}$$

while from (14)–(16) and the Casimir eigenvalue one has

$$j(j+1) = j(Q^{(j)2} + P^{(j)2}) + \left[H^{(j)} - \left(j + \frac{1}{2}\right) E^{(j)}\right]^2 \Rightarrow$$

$$\Rightarrow H^{(\infty)} = \frac{1}{2}(P^{(\infty)2} + Q^{(\infty)2}). \tag{43}$$

In this way the Hamiltonian generator acquires the standard form of a quantum harmonic oscillator, a quadratic function of the Heisenberg–Weyl generators.

In the $(2j{+}1)$-dimensional representation j, the rescaled operators (40) act on functions $F(\xi) := \Phi(q)$ of position $\xi := q/\sqrt{j}$ by shift operators through $1/\sqrt{j}$ as follows:

$$Q^{(j)}F(\xi) = \frac{1}{\sqrt{j}} Q\,\Phi(q) = \frac{q}{\sqrt{j}}\,\Phi(q) = \xi F(\xi), \tag{44}$$

$$P^{(j)}F(\xi) = -\frac{i}{2\sqrt{j}}\left[\alpha^j(-\sqrt{j}\,\xi)\,F\left(\xi{+}\frac{1}{\sqrt{j}}\right) - \alpha^j(\sqrt{j}\,\xi)\,F\left(\xi{-}\frac{1}{\sqrt{j}}\right)\right], \tag{45}$$

$$H^{(j)}F(\xi) = -\frac{1}{2j}\left[\alpha^j(-\sqrt{j}\,\xi)\,F\left(\xi{+}\frac{1}{\sqrt{j}}\right) + \alpha^j(\sqrt{j}\,\xi)\,F\left(\xi{-}\frac{1}{\sqrt{j}}\right)\right]. \tag{46}$$

When $j \to \infty$ with ξ remaining finite, (44) takes the standard form; assuming that $F(\xi+\epsilon) = F(\xi) + \epsilon\, F'(\xi) + \frac{1}{2}\epsilon^2\, F''(\xi) + \ldots$ holds for all «continuous» functions involved, then the limit of (45) is the usual derivative

$$\lim_{j\to\infty} P^{(j)} F(\xi) = -\lim_{j\to\infty} \frac{i\sqrt{j}}{2}\sqrt{1-\frac{\xi^2-1}{j}}\times \\ \times\left[F\left(\xi+\frac{1}{\sqrt{j}}\right) - F\left(\xi-\frac{1}{\sqrt{j}}\right)\right] = -i\frac{\partial}{\partial\xi}\, F(\xi), \quad (47)$$

and for (46) the limit involves second derivatives (cf. (43)), so that we obtain the standard realization of position and momentum, and the quantum harmonic oscillator Schrödinger equation.

3.6. Contraction of the Finite Oscillator Wavefunctions. It is well known that the binomial distribution becomes the Gaussian function when the number of points N grows while their separation decreases by $N^{-1/2}$. So the contraction of the $u(2)$ algebra should imply the $j \to \infty$ limit of the Kravchuk functions (26) to the well-known Hermite wavefunctions of the ordinary quantum oscillator. In fact, the original argument [19] for the contraction of Kravchuk to Hermite polynomials was phrased in terms of the limit of the point orthogonality measures. But to our knowledge, the limit of the functions has not yet been proven directly. This may be due to the fact that the usual representation of Kravchuk polynomials in terms of Gauss hypergeometric functions, Eq. (29), is ineligible to serve in this limit.

To prove directly that the Kravchuk functions (26) contract to the quantum harmonic oscillator wavefunctions when $j \to \infty$ and $n = m + j$ are kept finite (so $m \to -\infty$), instead of using limit relations for the ${}_2F_1$ functions, we use the expression in [28] for the d functions in terms of hypergeometric ${}_3F_2$ functions, which are valid for q integer,

$$\Phi_n^{(N)}(q) = \frac{(-1)^{n/2+q}}{\sqrt{\pi}\, j!}\sqrt{(j+q)!\,(j-q)!}\times \\ \times\begin{cases} \sqrt{\dfrac{\Gamma\left(\frac{n+1}{2}\right)\Gamma\left(j-\frac{n-1}{2}\right)}{\Gamma\left(\frac{n}{2}+1\right)\Gamma\left(j-\frac{n}{2}+1\right)}}\ {}_3F_2\left(\begin{matrix}-q, q, \frac{n+1}{2}\\ \frac{1}{2}, j+1\end{matrix}\middle| 1\right), & n \text{ even}, \\ \dfrac{2iq}{j+1}\sqrt{\dfrac{\Gamma\left(\frac{n}{2}+1\right)\Gamma\left(j-\frac{n}{2}+1\right)}{\Gamma\left(\frac{n+1}{2}\right)\Gamma\left(j-\frac{n-1}{2}\right)}}\ {}_3F_2\left(\begin{matrix}-q, q, \frac{n}{2}+1\\ \frac{3}{2}, j+2\end{matrix}\middle| 1\right), & n \text{ odd}. \end{cases} \quad (48)$$

With the mode number $n = j + m$ fixed and finite, and $q = \sqrt{j}\,\xi$ (so that the points ξ are integers divided by $\sqrt{j}$), the contraction limit $j \to \infty$ is

$$\lim_{j\to\infty}(-1)^q\, j^{1/4}\,\Phi_n^{(N)}(q) = \frac{(-2)^{n/2}}{\sqrt{\sqrt{\pi}\,n!}}\,\mathrm{e}^{\xi^2}\times$$
$$\times\begin{cases} \dfrac{\Gamma\left(\frac{n+1}{2}\right)}{\Gamma(\frac{1}{2})}\ {}_1F_1\left(\dfrac{n+1}{2};\dfrac{1}{2};-\xi^2\right), & n \text{ even},\\[2ex] 2i\xi\,\dfrac{\Gamma\left(\frac{n}{2}+1\right)}{\Gamma(\frac{1}{2})}\ {}_1F_1\left(\dfrac{n}{2}+1;\dfrac{3}{2};-\xi^2\right), & n \text{ odd}. \end{cases} \tag{49}$$

Using the relation ${}_1F_1(\alpha;\gamma,z) = \mathrm{e}^z\,{}_1F_1(\gamma-\alpha;\gamma,-z)$ between two confluent hypergeometric functions, and comparing with a standard expression for Hermite polynomials in [29], when $q=\sqrt{j}\,\xi$, we obtain

$$\lim_{j\to\infty}(-1)^q\, j^{1/4}\,\Phi_n^{(N)}(q) = \lim_{j\to\infty}(-1)^{n+j}\, j^{1/4}\, d^j_{n-j,q}\left(\frac{1}{2}\pi\right) =$$
$$= \frac{\mathrm{e}^{-\xi^2/2}}{\sqrt{\sqrt{\pi}2^n\,n!}}H_n(\xi) =: \Psi_n(\xi). \tag{50}$$

The $\Psi_n(\xi)$ are of course the wavefunctions of the one-dimensional quantum oscillator, for $n|_0^\infty$, and $\xi\in\Re$.

4. FINITE TWO-DIMENSIONAL OSCILLATOR

The simplest two-dimensional generalization of the one-dimensional finite oscillator of the previous Section, is a square grid of $(N{+}1)\times(N{+}1)$ points, with the algebra $u(1)\oplus su(2)^{(x)}\oplus su(2)^{(y)}$ of two independent and mutually commuting subalgebras (14)–(17) for the x and y directions and the same central algebra $u(1)$ of generator $E_J^{(x)} = E_J^{(y)} = \dfrac{1}{2}N\hat{1}$; this *Cartesian* pattern can be generalized straightforwardly to any dimension D, as we remark in the first Subsection. But dimension $D=2$ is special because $su(2)^{(x)}\oplus su(2)^{(y)} = so(4)$, and the generators of the two $su(2)$'s (see (18)) combine into $so(4)$ generators $\Lambda_{j,k}$, now for $1\leqslant j<k\leqslant 4$, as follows:

$$\begin{array}{|c|c|}\hline J_3^{(x)} & -J_2^{(x)}\\ \hline & J_1^{(x)}\\ \hline\end{array}\ \oplus\ \begin{array}{|c|c|}\hline J_3^{(y)} & -J_2^{(y)}\\ \hline & J_1^{(y)}\\ \hline\end{array}\ =\ \begin{array}{|c|c|c|}\hline J_3^{(x)}+J_3^{(y)} & -J_2^{(x)}-J_2^{(y)} & J_1^{(x)}-J_1^{(y)}\\ \hline & J_1^{(x)}+J_1^{(y)} & J_2^{(x)}-J_2^{(y)}\\ \hline & & J_3^{(x)}-J_3^{(y)}\\ \hline\end{array} \tag{51}$$

We work here with the further restriction that the representation of $so(4)$ be of the *symmetric* (or *most degenerate*) kind, whose two commuting $so(3)$ Casimir operators are bound by

$$(\mathbf{J}^{(x)})^2 = E_J(E_J + \hat{1}) = (\mathbf{J}^{(y)})^2. \tag{52}$$

As we saw in Sec. 2, Eqs. (4), (5), *angular momentum* can be placed naturally in algebra chain $so(4) \supset so(3) \supset so(2)$. After the first Subsection, we shall return to this Gel'fand–Tsetlin chain, that corresponds to a finite oscillator with sensor-points placed along radial and angular coordinates.

4.1. Cartesian Positions, Modes and Wavefunctions. We can build the Kronecker eigenbasis of positions (20) for a finite two-dimensional oscillator arranged in an x–y square Cartesian grid, straightforwardly:

$$Q_x \,|N; q_x, q_y\rangle_1 \;=\; q_x \,|N; q_x, q_y\rangle_1, \qquad q_x|_{-N/2}^{N/2}, \tag{53}$$

$$Q_y \,|N; q_x, q_y\rangle_1 \;=\; q_y \,|N; q_x, q_y\rangle_1, \qquad q_y|_{-N/2}^{N/2}, \tag{54}$$

$$(\mathbf{J}^{(x)})^2 \,|N; q_x, q_y\rangle_1 = \frac{1}{2}N\left(\frac{1}{2}N + 1\right) \,|N; q_x, q_y\rangle_1 = (\mathbf{J}^{(y)})^2 \,|N; q_x, q_y\rangle_1. \tag{55}$$

These $(N{+}1)^2$ positions are shown in Fig. 4 (left).

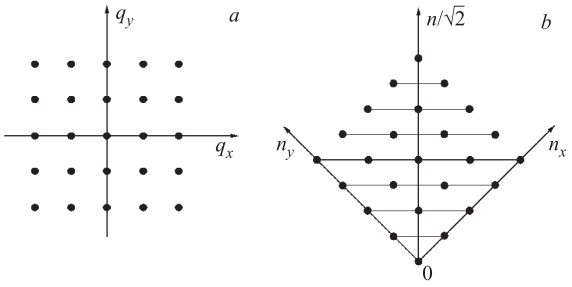

Fig. 4. *a*) The positions of sensor-points in the Cartesian finite oscillator. *b*) States classified by total number and difference of quanta along the x and y axes

Similarly, we can build the *Cartesian modes* of the finite two-dimensional oscillator as direct products $|N; n_x, n_y\rangle_H = |N, n_x\rangle_{H_x} \,|N, n_y\rangle_{H_y}$,

$$\begin{aligned} H_x \,|N; n_x, n_y\rangle_H &= \left(n_x + \frac{1}{2}\right) \,|N; n_x, n_y\rangle_H, \qquad n_x|_0^N, \\ H_y \,|N; n_x, n_y\rangle_H &= \left(n_y + \frac{1}{2}\right) \,|N; n_x, n_y\rangle_H, \qquad n_y|_0^N. \end{aligned} \tag{56}$$

They can be arranged into a rhombus pattern, vertical axis counts the total number of quanta,

$$n := n_x+n_y, \quad H\,|N;n_x,n_y\rangle_H = (n+1)\,|N;n_x,n_y\rangle_H, \quad H := H_x+H_y, \tag{57}$$

and the horizontal axis counts their difference. These $(N+1)^2$ points are shown in Fig. 4, *a*.

The *Cartesian mode* wavefunctions of the two-dimensional finite oscillator are then the product of two one-dimensional ones,

$$\Phi^{(N)}_{n_x,n_y}(q_x,q_y) := {}_1\langle N;q_x,q_y|N;n_x,n_y\rangle_H = \Phi^{(N)}_{n_x}(q_x)\,\Phi^{(N)}_{n_y}(q_y). \tag{58}$$

Returning to the pattern of $so(4)$ states in Fig. 4, *b*, we may be tempted to think that the energy degeneracy of the states

$$\Big\{\,|N;0,n\rangle_H,\ |N;1,n-1\rangle_H,\ldots,\ |N;n,0\rangle_H\Big\}, \quad n|_0^N, \tag{59}$$

$$\Big\{\,|N;n{-}N,N\rangle_H,\ |N;n{-}N{+}1,N{-}1\rangle_H,\ldots,\ |N;N,n{-}N\rangle_H\Big\}, \quad n|_N^{2N} \tag{60}$$

indicates some higher symmetry for the finite oscillator, as it does for the «continuous» two-dimensional quantum oscillator which has the larger symmetry group $U(2)$. There, the centre $U(1)_c \subset U(2)$ is generated by the total number-of-quanta operator. But within $SO(4)$, the states with the same energy are *not* connected into multiplets by a subalgebra of generators.

The continuum model includes continuous *rotations* of the oscillator position plane around its origin [31], but the finite oscillator does *not*. Yet, one can introduce *imported* symmetries [32] into the finite oscillator model through linear combinations with coefficients taken from the continuous model states $|N;n_x,n_y)$ that rotate under the orbital angular momentum operator $2L_3 := (Q_xP_y - Q_yP_x)$ [31]. This was done in [8] to produce finite analogues of states with definite angular momentum, and unitary transformations $\mathcal{R}(\theta)$ of the finite wavefunction set,

$$\mathcal{R}(\theta)\ |N;n_x,n_y\rangle_H := \sum_{n'_x+n'_y=n} |N;n'_x,n'_y\rangle_H\, R^{(n)}_{\frac{1}{2}(n'_y-n'_x),\frac{1}{2}(n_x-n_y)}(\theta), \tag{61}$$

$$R^{(n)}_{\kappa',\kappa}(\theta) := (N;n'_x,n'_y|\,\mathrm{e}^{-2i\theta L_3}\,|N;n_x,n_y) = (-i)^{\kappa'-\kappa}\,d^{n/2}_{\kappa',\kappa}(2\theta), \tag{62}$$

$$n = \begin{cases} n_x+n_y, & \text{when} \quad 0 \leqslant n_x+n_y \leqslant N, \\ 2N-n_x-n_y, & \text{when} \quad N \leqslant n_x+n_y \leqslant 2N. \end{cases} \tag{63}$$

These «rotations» acting on finite oscillator wavefunctions $|N;n_x,n_y\rangle_H$'s, are thus block-diagonal in n.

4.2. The $so(4)$ Algebra of the Finite Radial Oscillator. Besides Cartesian coordinates, the harmonic oscillator separates also in polar coordinates [30]. To describe this coordinate set on the group-theoretical basis of the $so(4)$ algebra for the finite oscillator, we return to the notation and box diagram for the orthogonal algebra generators in (18) and (51), $\Lambda_{j,k}$, again for $1 \leqslant j < k \leqslant 4$, with commutation relations (5) and the *new* asignments for the physical observables to the $so(4)$ generators [9]:

$$\begin{array}{|c|c|c|}\hline \Lambda_{1,2} & \Lambda_{1,3} & \Lambda_{1,4} \\ \hline & \Lambda_{2,3} & \Lambda_{2,4} \\ \cline{2-3} & & \Lambda_{3,4} \\ \cline{3-3}\end{array} = \begin{array}{|c|c|c|}\hline J & P_x & P_y \\ \hline & Q_x & Q_y \\ \cline{2-3} & & M \\ \cline{3-3}\end{array}, \qquad \begin{array}{l} J := H - E_J - \hat{1} \text{ mode}, \\ M \text{ — angular momentum.}\end{array} \tag{64}$$

In this pattern we see the following desirable properties: angular momentum M and mode (shifted energy) J commute; position (Q_x, Q_y) and momentum (P_x, P_y) transform as 2-vectors under angular momentum M; and x-phase space (Q_x, P_x) and y-phase space (Q_y, P_y) rotate similarly under the Hamiltonian and J. On the other hand, there are also new nonstandard commutators $[Q_x, Q_y]$ and $[P_x, P_y]$, anticipated in Eqs. (8), that generalize (19) to two dimensions. Finally, as in the Cartesian case of the previous Subsection, the model is restricted to the symmetric $so(4)$ representations, where the two independent second-degree Casimir operators are

$$\mathcal{C} = \sum_{j,k} \Lambda_{j,k}\, \Lambda_{j,k} = N(N+2), \quad \text{where } N := 2j, \tag{65}$$

$$\mathcal{D} = \sum_{j,k,l} \Lambda_{j,k} \Lambda_{l,4} = 0. \tag{66}$$

Hence the value of $N = 2j \in \{0, 1, 2, \ldots\}$ is sufficient to characterize the symmetric $so(4)$ irreps, whose dimension is $(N+1)^2$.

4.3. States of Mode and Angular Momentum. The eigenbasis of the two commuting $so(4)$ generators

$$J = \Lambda_{1,2} = J_3^{(x)} + J_3^{(y)}, \quad M = \Lambda_{3,4} = J_3^{(x)} - J_3^{(y)}, \tag{67}$$

(see (51) and (64)) is the set of finite radial oscillator states classified by (displaced) energy and angular momentum by the subalgebra chains $so(4) \supset so(2)_J \oplus so(2)_M \simeq u(1)^{(x)} \oplus u(1)^{(y)}$. When $J_3^{(x)}$ and $J_3^{(y)}$ have eigenvalues $m_x|_{-j}^{j}$ and $m_y|_{-j}^{j}$, respectively, the eigenstates will be denoted

$$J\ |N;\nu,m\rangle_{JM} = \nu\ |N;\nu,m\rangle_{JM}, \tag{68}$$

$$\nu = m_x + m_y \in \{-N, -N+1, \ldots, N\}, \tag{69}$$

$$M\ |N;\nu,m\rangle_{JM} = m\ |N;\nu,m\rangle_{JM}, \tag{70}$$

$$m = m_x - m_y \in \{-N+|\nu|, -N+|\nu|+2, \ldots, N-|\nu|\} \tag{71}$$

for a fixed value of (displaced) energy ν. These states have

$$\begin{aligned} &\text{energy } E_\nu = N + \nu + 1 = 2n + |m| + 1, \text{ where} \\ &\text{radial mode number } n := \frac{1}{2}(N + \nu - |m|) \in \{0, 1, \ldots, 2N\}. \end{aligned} \tag{72}$$

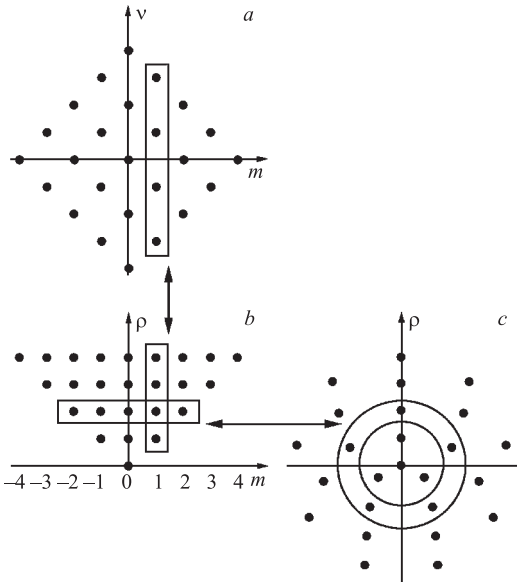

Fig. 5. *a*) States of the finite radial oscillator classified by angular momentum m and displaced energy ν for $j = 2$ ($N = 4$ with a total of 25 states). *b*) The same set of states classified by angular momentum m and radial position ρ; the boxes joined by the arrow represent states which are linear combinations of the others. *c*) The same states, where for each radius ρ a finite Fourier transform is performed between its $2\rho+1$ angular momentum states to produce states of definite radius and angle (up to independent rotation of the circles)

In Fig. 5, *a* we arrange these states in a rhombus pattern, which is the same as of Fig. 4, *b* for the energy and angular momentum states of the finite Cartesian oscillator. Figure 5, *b*, *c* will be explained below.

4.4. States of Definite Radius and Angular Momentum. The $so(4)$ oscillator model can be Cartesian or radial, depending on our choice of the eigenbasis associated to operators of position. We use the box patterns to define two subalgebras:

$$\begin{array}{|c|c|c|}\hline S_3 & -S_2 & S_1 \\ \hline & R_1 & R_2 \\ \cline{2-3} & & R_3 \\ \cline{3-3}\end{array} = \begin{array}{|c|c|c|}\hline J & P_x & P_y \\ \hline & Q_x & Q_y \\ \cline{2-3} & & M \\ \cline{3-3}\end{array} = \begin{array}{|c|c|c|}\hline L_3 & -L_2 & K_1 \\ \hline & L_1 & K_2 \\ \cline{2-3} & & K_3 \\ \cline{3-3}\end{array} \tag{73}$$

We characterize the finite radial oscillator model by the subalgebras

$$so(4) \supset so(3)_R \;\; = \text{span}\,\{R_1, R_2, R_3\} \qquad \text{of } \textit{position}, \tag{74}$$

$$so(4) \supset so(3)_{GT} = \text{span}\,\{L_1, L_2, L_3\} \qquad \text{Gel'fand–Tsetlin} \tag{75}$$

with the commutation relations:

$$[R_j, R_k] = i\epsilon_{jkl} R_l, \quad [R_j, S_k] = i\epsilon_{jkl} S_l, \quad [S_j, S_k] = i\epsilon_{jkl} R_l, \tag{76}$$

$$[L_j, L_k] = i\epsilon_{jkl} L_l, \quad [L_j, K_k] = i\epsilon_{jkl} K_l, \quad [K_j, K_k] = i\epsilon_{jkl} L_l. \tag{77}$$

Since $\mathbf{L} = \mathbf{J}^{(x)} + \mathbf{J}^{(y)}$, the Gel'fand–Tsetlin chain containing $so(3)_{GT}$ conforms to the direct sum decomposition (51), so its irreducible representations ℓ in the symmetric representation N of $so(4)$ are the *coupling* of two angular momenta $j = \dfrac{1}{2}N$ to the total angular momentum $\ell \in \{0, 1, \ldots, N\}$. On the other hand, the *radial* subalgebra chain $so(4) \supset so(3)_R \supset so(2)_M$ is characterized by the eigenvalues of

$$(\mathbf{R})^2 := R_1^2 + R_2^2 + R_3^2, \quad \text{spectrum:} \quad \rho(\rho+1),\ \rho \in \{0, 1, \ldots, N\}, \tag{78}$$

$$\text{and in each irrep } \rho, \quad R_3, \quad \text{spectrum:} \quad m \in \{-\rho, -\rho+1, \ldots, \rho\}. \tag{79}$$

4.5. The Finite Oscillator Radial Wavefunctions. The total number of independent states in (79) is $\sum_{\rho=0}^{N}(2\rho+1) = (N+1)^2$, matching the dimension of the $so(4)$ representation space $N = 2j$. We denote the finite oscillator eigenstates of $(\mathbf{R})^2$ and R_3 by $|N; \rho, m\rangle_R$, and in Fig. 5, *b* we show them rearranged with respect to the *radius* ρ and *angular momentum* m, as we now proceed to detail.

We now build finite oscillator radial wavefunctions as the overlaps between the mode basis (68)–(71) and the radial basis of (78), (79). In the canonical Gel'fand–Tsetlin basis, this is

$$\mathbf{L}^2\,|N; \ell, \mu\rangle_{GT} = (\mathbf{J}^{(x)} + \mathbf{J}^{(y)})^2\,|N; \ell, \mu\rangle_{GT} = \ell(\ell+1)\,|N; \ell, \mu\rangle_{GT}, \quad \ell|_0^N, \tag{80}$$

$$L_3\,|N; \ell, \mu\rangle_{GT} = (J_3^{(x)} + J_3^{(y)})\,|N; \ell, \mu\rangle_{GT} = \mu\,|N; \ell, \mu\rangle_{GT}, \quad \mu|_{-\ell}^{\ell}. \tag{81}$$

The overlaps between the JM- and the Gel'fand–Tsetlin kets are thus the ordinary $su(2) = so(3)$ Clebsch–Gordan coefficients [18, 33, 34],

$$C^{\frac{1}{2}N,\frac{1}{2}N,\ell}_{\frac{1}{2}(\nu+m),\frac{1}{2}(\nu-m),\mu} = {}_{GT}\langle N;\ell,\mu|N;\nu,m\rangle_{JM}. \tag{82}$$

We must now relate the Gel'fand–Tsetlin chain to the chain containing the radial position subalgebra of Eqs. (78), (79), exchanging the indices $1 \leftrightarrow 4$ and $2 \leftrightarrow 3$ in the pattern (73) by means of the $SO(4)$ transformation

$$T(\chi) := \mathrm{e}^{-i\chi(\Lambda_{2,3}-\Lambda_{1,4})} = \mathrm{e}^{-2i\chi J_1^{(b)}}, \text{ for } \chi = \pm\frac{1}{2}\pi. \tag{83}$$

This intertwines the generators as

$$T\left(\frac{1}{2}\pi\right)\begin{pmatrix} L_1,\ L_2,\ L_3 \\ K_1,\ K_2,\ K_3 \end{pmatrix} T\left(\frac{1}{2}\pi\right)^{-1} = \\ = \begin{pmatrix} L_1,\ K_2,\ K_3 \\ K_1,\ L_2,\ L_3 \end{pmatrix} = \begin{pmatrix} R_1,\ R_2,\ R_3 \\ S_1,\ S_2,\ S_3, \end{pmatrix}, \tag{84}$$

$$T\left(\frac{1}{2}\pi\right)\begin{pmatrix} J_1^{(x)}, & J_2^{(x)}, & J_3^{(x)} \\ J_1^{(y)}, & J_2^{(y)}, & J_3^{(y)} \end{pmatrix} T\left(\frac{1}{2}\pi\right)^{-1} = \\ = \begin{pmatrix} J_1^{(x)}, & J_2^{(x)}, & J_3^{(x)} \\ J_1^{(y)}, & -J_2^{(y)}, & -J_3^{(y)} \end{pmatrix}, \tag{85}$$

and the Gel'fand–Tsetlin and mode bases as

$$T\left(\frac{1}{2}\pi\right)|N;\ell,\mu\rangle_{GT} = |N;\ell,\mu\rangle_R,\ T\left(\frac{1}{2}\pi\right)|N;\nu,m\rangle_{JM} = |N;m,\nu\rangle_{JM}. \tag{86}$$

The finite radial oscillator wavefunctions, being the overlap between the radial position and angular momentum bases with the same energy, are thus given by a Clebsch–Gordan coefficient:

$$(-1)^\rho \Phi^{(N)}_{\nu,m}(\rho) := {}_R\langle N;\rho,m|N;m_x{+}m_y,m_x{-}m_y\rangle_{JM} = \tag{87}$$
$$= {}_{GT}\langle N;\rho,m|N;m_x{-}m_y,m_x{+}m_y\rangle_{JM} = \tag{88}$$
$$= C^{j,j,\rho}_{m_x,-m_y,m} = C^{j,j,\rho}_{\frac{1}{2}(m+\nu),\frac{1}{2}(m-\nu),m}, \tag{89}$$

where we use as before $N = 2j$, $\nu = m_x{+}m_y$ and $m = m_x{-}m_y$, where $|m| \leqslant \rho \leqslant N$ are integers, and where their ranges are determined by the nonzero values of these coefficients, viz.,

$$\text{for } \nu|^N_{-N} \text{ fixed}, \qquad m \in \{-N{+}|\nu|, -N{+}|\nu|{+}2, \ldots, N{-}|\nu|\}; \tag{90}$$
$$\text{for } m|^N_{-N} \text{ fixed}, \qquad \nu \in \{-N{+}|m|, -N{+}|m|{+}2, \ldots, N{-}|m|\}. \tag{91}$$

We note that the sign $(-1)^\rho$ in (91) appears because the standard $su(2)$ Clebsch–Gordan coefficients have been traditionally defined from the requirement that the *highest* state have no changes of sign between neighboring values of ρ, while here we are asking for the same condition for the *ground* state of the oscillator.

4.6. Discrete Radii and Discrete Angles. As we can see in Fig. 5, *a*, for fixed angular momentum m, there are $N - |m|$ independent wavefunctions (89), distinguished by $\nu \in \{-N+|m|, -N+|m|+2, \ldots, N-|m|\}$; these are functions of the same number $N-|m|$ of radii $\rho|_{|m|}^{N}$. For each m, the wavefunctions are real and form an orthonormal and complete set, corresponding to the known bilinear sums of Clebsch–Gordan coefficients [18, Sec. 8.7.2]:

$$\sum_{\nu=-N+|m|:\,(+2)}^{N-|m|} \Phi_{\nu,m}^{(N)}(\rho)\Phi_{\nu,m}^{(N)}(\rho') = \delta_{\rho,\rho'}, \qquad \sum_{\rho=|m|}^{N} \Phi_{\nu,m}^{(N)}(\rho)\Phi_{\nu',m}^{(N)}(\rho) = \delta_{\nu,\nu'}. \quad (92)$$

The sum notation «: $(+2)$» indicates that the values of ν are spaced by 2.

Having formed the linear combinations of states of definite radius in Fig. 5, *b*, we see that for a fixed value of the radius $\rho|_0^N$, the angular momenta can have the $2\rho+1$ values $m \in \{-\rho, -\rho+1, \ldots, \rho\}$. Because of (70) and (79), for each ρ the set of angular momentum states will be orthogonal and complete:

$${}_R\langle N;\rho,m|N;\rho,m'\rangle_R = \delta_{m,m'}, \qquad \sum_{m=-\rho}^{\rho} |N;\rho,m\rangle_{R\,R}\langle N;\rho,m| = \hat{1}_\rho, \quad (93)$$

where $\hat{1}_\rho$ is the unit operator in each space of definite ρ. Now, for every one, fixed radius, the natural Hilbert space is that of functions on the circle or, since there are a finite number of m's, $2\rho+1$ points equidistant on a circle, as defined by the common discrete Fourier transform [35, Part I]. Now, for each ρ we introduce the discrete angles (to be also used as *labels*),

$$\theta_k = \frac{2\pi k}{2\rho+1}, \quad k \in \{-\rho, -\rho+1, \ldots, \rho\}, \quad (94)$$

and thus define new *radius-and-angle* kets by

$$|N;\rho,\theta_k\rangle_\circ \;:=\; \frac{1}{\sqrt{2\rho+1}} \sum_{m=-\rho}^{\rho} \mathrm{e}^{im\theta_k}\, |N;\rho,m\rangle_R, \quad (95)$$

$$|N;\rho,m\rangle_R \;=\; \frac{1}{\sqrt{2\rho+1}} \sum_{k=-\rho}^{\rho} \mathrm{e}^{-im\theta_k}\, |N;\rho,\theta_k\rangle_\circ. \quad (96)$$

This basis of states for the circle of radius ρ is also orthogonal and complete in the index k of θ_k; they are cyclic functions of θ_k modulo 2π (or of k modulo N).

We interpret θ straightforwardly as the angle coordinate in the point array shown in Fig. 5, *c*. This we call the *finite polar array*; the finite radial oscillator wavefunctions will be assumed to be measured by discrete sensors on the points of this set.

At the centre $\rho = 0$ of the finite polar array of Fig. 5, *c*, there is only one state $m = 0$, and one irrelevant angle θ_0; its only state is $|N; 0, \theta_0\rangle_\circ = |N; 0, 0\rangle_R$. On the first circle $\rho = 1$, there can be three states, $m = 0$ and $m = \pm 1$; correspondingly in the figure there are three points on the circle, of angles $\theta_0 = 0$ and $\theta_{\pm 1} = \pm\dfrac{2}{3}\pi$. On the following circles, of radii $\rho = 2, 3, \ldots$, there will be $2\rho+1$ points, sensors or pixels around each circle. And finally, there is a maximal circle $\rho = N$ with the maximal number $2N+1$ of angular momentum states and of points around that circle.

It should be remarked that the finite polar array presents an — almost — homogeneous density of points. The discrete surface element in polar coordinates is measured by $\Delta^2\mathbf{r} := \rho\,\Delta\rho\,\Delta\theta_k$. The polar array has $\Delta\rho = 1$ and $\Delta\theta_k = \theta_k - \theta_{k-1} = 2\pi/(2\rho+1)$, so it will have a density $\pi\rho/(\rho + 1/2)$ which, as ρ grows, rather quickly becomes π.

4.7. Clebsch–Gordan Coefficients and Dual Hahn Polynomials. Clebsch–Gordan coefficients can be written in terms of the ${}_3F_2$ hypergeometric function (see [18, Eq. 8.5.2(21)]), with the equivalent notation $C^{j,j,\rho}_{m_x,-m_y,m} \equiv C^{\rho,m}_{j,m_x;j,-m_y}$, and as usual $j = \dfrac{1}{2}N$,

$$
\begin{aligned}
\Phi^{(N)}_{\nu,m}(\rho) &= \frac{(-1)^\rho\,\rho!}{\left(\rho - j + \dfrac{\nu+m}{2}\right)!\,\left(\rho - j + \dfrac{\nu-m}{2}\right)!} \times \\
&\times \sqrt{\frac{\left(j+\dfrac{\nu+m}{2}\right)!\,\left(j+\dfrac{\nu-m}{2}\right)!\,(\rho+m)!\,(\rho-m)!\,(2\rho+1)}{\left(j-\dfrac{\nu+m}{2}\right)!\,\left(j-\dfrac{\nu-m}{2}\right)!\,(2j-\rho)!\,(2j+\rho+1)!}} \times \\
&\times {}_3F_2\left(\begin{matrix} -2j+\rho,\ -j+\dfrac{\nu+m}{2},\ -j+\dfrac{\nu-m}{2} \\ -j+\dfrac{\nu-m}{2}+\rho+1,\ -j+\dfrac{\nu+m}{2}+\rho+1 \end{matrix}\,\middle|\, 1\right), \qquad (97) \\
&= (-1)^{2j-n}\frac{(2j)!}{m!}\sqrt{\frac{(2\rho+1)\,(n+m)!\,(2j-n-m)!\,(\rho+m)!}{n!\,(2j-n)!\,(\rho-m)!\,(2j-\rho)!\,(2j+\rho+1)!}} \times \\
&\times {}_3F_2\left(\begin{matrix} -n,\ -\rho,\ \rho+1 \\ m+1,\ -2j \end{matrix}\,\middle|\, 1\right), \qquad (98)
\end{aligned}
$$

where the radial mode number $n = \frac{1}{2}(N+\nu-m) = j+m_y$ determines the degree of the ${}_3F_2$ function of unit argument, which is a *dual Hahn polynomial* [29,36–38] in the variable $\rho(\rho+1)$,

$$R_n\left(\lambda_{(\rho)}; m, m', N\right) := {}_3F_2\left(\left.\begin{matrix}-n,\ -\rho,\ \rho+m+m'+1 \\ m+1,\ -N\end{matrix}\right| 1\right), \quad (99)$$

$$\lambda_{(\rho)} = \rho(\rho+m+m'+1). \quad (100)$$

The factor in front of this polynomial in the wave function (97) is the square root of the dual-Hahn orthogonality measure.

The polynomial factor of (97), (98) allows a natural analytic continuation to the ρ-complex plane; the orthogonality measure is also analytic; it is positive within the orthogonality interval, becomes zero one unit beyond, and is negative thereafter. The wavefunctions are thus analytic in the radius ρ on the open interval

$$\max\left(|m|-1, -1/2\right) < \rho < N+1, \quad (101)$$

with branch zeros at the endpoints. Hence, finite systems *can* be asigned with a «continuous» position coordinate that permits the dynamical algebra to be realized by *difference operators* that bind any three points of the position variable separated by units, within (and one unit outside) the interval. Hence there exists a Schrödinger difference equation to rule over finite systems [5, 20, 39].

In the previous expressions it is manifested that the oscillator states $\Phi^{(N)}_{\nu,m}(\rho)$ are even functions of angular momentum m, namely $\Phi^{(N)}_{\nu,m}(\rho) = \Phi^{(N)}_{\nu,-m}(\rho)$, corresponding to the symmetry relation of the Clebsch–Gordan coefficients $C^{j,j,\rho}_{m_x,-m_y,m} = C^{j,j,\rho}_{m_y,-m_x,-m}$. In what follows we will consider only positive values of m. In Fig. 5, *b* we showed the linear combinations of finite oscillator states that map between the mode and the radius bases, for fixed angular momentum m. The finite radial oscillator wavefunctions $\Phi^{(N)}_{\nu,m}(\rho)$ in (87)–(97) are shown in Fig. 6, where we plot the lowest-, middle-, and highest-energy states. The lowest ones ($\nu \approx -N$) do resemble the ordinary quantum radial wavefunctions, multiplied by the root of the radial measure $\sqrt{r}$. The highest ones ($\nu \approx N$) have the same envolvent as the lowest ones, but alternate sign between every two points (due to $C^{j,j,\rho}_{m_x,m_y,m} = (-1)^\rho C^{j,j,\rho}_{m_y,m_x,m}$, relating $\pm\nu$). The middle radial states $\nu = 0$ resemble the right half of the middle 1-dim oscillator Kravchuk function in Fig. 2 and highlight that the wavefunctions exist only for radii $\rho \geqslant |m|$.

4.8. Finite-Difference Radial Schrödinger Equation. The three-term recurrence relation $C^{j,j,\rho}_{m_x,-m_y,m}$ for the Clebsch–Gordan coefficient and its neighbouring $C^{j,j,\rho\pm1}_{m_x,-m_y,m}$ [18, Eq. 8.6.5(27)] (or the difference equation satisfied by the

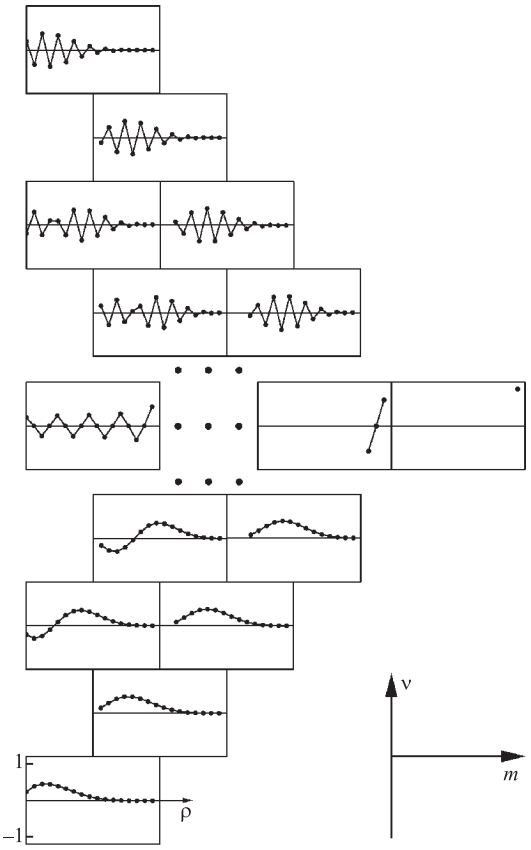

Fig. 6. Finite radial oscillator wavefunctions for $j = 8$ ($N = 16$ and hence 17 points). From bottom to top, for increasing energy $\nu = 2n + |m| + 1 \in \{0, 1, 2, 3, \ldots, 7, 8\}$. The wavefunctions exist in the range $|m| \leqslant \rho \leqslant N$. We interpolate points by lines for better visibility

Hahn polynomials [38, Eq. (1.6.5)]), imply that

$$(m_x + m_y)\, C^{j,j,\rho}_{m_x,-m_y,m} = \\ = \sqrt{\frac{(\rho+m+1)(\rho-m+1)(2j-\rho)(2j+\rho+2)}{(2\rho+1)(2\rho+3)}}\, C^{j,j,\rho-1}_{m_x,-m_y,m} + \\ + \sqrt{\frac{(\rho+m)(\rho-m)(2j-\rho+1)(2j+\rho+1)}{(2\rho+1)(2\rho-1)}}\, C^{j,j,\rho+1}_{m_x,-m_y,m}. \quad (102)$$

From here results the finite ($N = 2j$) radial oscillator Hamiltonian and finite-difference radial Schrödinger equation for the interval $\max(|m|-1, -1/2) < \rho < N+1$, as determined in (101):

$$H^j_m(\rho) = -\frac{1}{2}[\alpha^j_m(\rho)\,\mathrm{e}^{-\partial_\rho} + (2j+1) + \mathrm{e}^{+\partial_\rho}\alpha^j_m(\rho)], \tag{103}$$

$$\alpha^j_m(\rho) := \sqrt{\frac{(\rho^2 - m^2)[(N+1)^2 - \rho^2]}{(\rho^2 - 1/4)}} = \alpha^j_m(-\rho) = \alpha^j_{-m}(\rho), \tag{104}$$

$$H^j_m(\rho)\Phi^{(N)}_{\nu,m}(\rho) = E_\nu \Phi^{(N)}_{\nu,m}(\rho), \text{ where } E_\nu = N + \nu + 1 = 2n + |m| + 1 \tag{105}$$

are the energies of the two-dimensional finite oscillator states $\Phi^{(N)}_{\nu,m}(\rho)$, which depend on the displaced principal quantum number ν (cf. (31)–(33)). Orthogonality and completeness relations stem from the bilinear sum rules for the Clebsch–Gordan coupling coefficients.

4.9. Finite Radial Oscillator Equivalent Potential. In continuum quantum mechanics, the Schrödinger equation and wavefunctions of the two-dimensional oscillator separate in polar coordinates (r, ϕ) into an angular part $\sim \mathrm{e}^{im\phi}$ with integer eigenvalues m and having $|m|$ nodal diameters, and a radial part $\sim L^{(m)}_n(r^2)$ having n nodal circles; the energy is then $E_\nu = 2n + |m| + 1$. The angular part contributes with a «centrifugal potential» summand $|m|/r^2$ to the radial Schrödinger equation. The finite radial oscillator Hamiltonian (103) does not obviously separate into a kinetic and potential energy parts, so again we search for an *equivalent potential* with the particular aim of recognizing this centrifugal term.

We can apply again the reconstruction of the potential out of nodeless solutions to the Schrödinger equation as in (35)–(38). The functions of radial mode number $n = 0$ have a dual-Hahn polynomial factor which is unity, while the factor of (98) with the lowest allowed energy for angular momentum m, $\nu_m := -2j + |m|$ at the boundary diagonals of Fig. 5, *a* is (for ρ and m integer)

$$\Phi^{(N)}_{\nu_m,m}(\rho) = (-1)^{2j}\sqrt{\frac{(2\rho+1)\,(2j)!\,(2j-m)!\,(\rho+m)!}{m!\,(2j-\rho)!\,(2j+\rho+1)!\,(\rho-m)!}}. \tag{106}$$

As in (37), the equivalent potential $V_{|m|}(\rho)$ for angular momentum m is found from the second difference of the previous functions within the analyticity interval (101),

$$V(\rho) - E_{\nu_m} + 1 = \frac{\Phi^{(N)}_{\nu_m,m}(\rho+1) + \Phi^{(N)}_{\nu_m,m}(\rho-1)}{2\Phi^{(N)}_{\nu_m,m}(\rho)} = \tag{107}$$

$$= \frac{1}{2}\left(\sqrt{\frac{(2\rho+3)(\rho+|m|+1)(2j-\rho)}{(2\rho+1)(\rho-|m|+1)(2j+\rho+2)}}+ \right.$$
$$\left. +\sqrt{\frac{(2\rho-1)(\rho-|m|)(2j+\rho+1)}{(2\rho+1)(\rho+|m|)(2j-\rho+1)}}\right), \qquad (108)$$
$$\max(|m|-1,-1/2)<\rho<2j+1.$$

Radial equivalent potentials are shown in Fig. 7 for various values of angular momentum m.

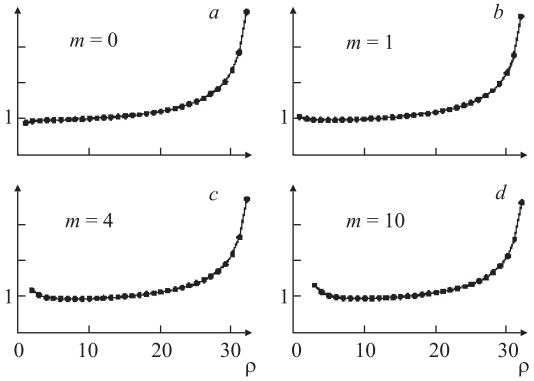

Fig. 7. Finite radial oscillator equivalent potentials for $j = 16$ ($N = 32$ and hence 33 points), for $m = 0, 1$ (*a*, *b*) and $m = 4, 10$ (*c*, *d*). The wavefunctions exist for $|m| \leqslant \rho \leqslant N$, so in the case $m = 0$ we have omitted the first point $\rho = 0$ because the second difference of the wavefunction addresses the nonexistent point $\rho = -1$

4.10. Contraction of the Finite Radial Oscillator Algebra. The finite radial oscillator model has a well-defined contraction limit to the ordinary quantum radial oscillator when the number and density of radial circles in position space increase without bound [40]. This was proven on the level of the algebras, $u(1)\oplus so(4) \to \mathrm{osc}_2 = \mathrm{span}\{\mathbf{Q}, \mathbf{P}, \hat{1}, \hat{H}, \hat{M}\}$ in [9] (see the pattern (64)). Essentially, one lets $2j = N \to \infty$ after changing the scale of position and momentum, while leaving intact energy and angular momentum,

$$\mathbf{Q}^{(j)} = \mathbf{Q}/\sqrt{j}, \qquad \mathbf{P}^{(j)} = \mathbf{P}/\sqrt{j}, \qquad (109)$$
$$E_J^{(j)} = j\hat{1}, \quad H^{(j)} = J + (2j+1)\hat{1}, \quad M^{(j)} = M. \qquad (110)$$

There are $N+1$ points in the symmetric interval of length $2\sqrt{j}$ with separation $1/\sqrt{j}$, while the energy levels remain separated by unity, and the rhombus of Fig. 5, *a* becomes the usual two-dimensional oscillator spectrum.

The noncanonical $so(4)$ commutators, Eqs. (8), become the usual ones of the Heisenberg–Weyl algebra. From the Casimir operators (65) and (66) we find the limit forms

$$H = \frac{1}{2}(\mathbf{P}^2 + \mathbf{Q}^2), \quad M = Q_x P_y - Q_y P_x, \quad \mathcal{C} = |\mathbf{Q}\,|^2, \tag{111}$$

as expected.

4.11. Contraction of the Wavefunctions. To find the limit of the finite radial oscillator wavefunctions when $N \to \infty$, we let the $so(4)$ multiplet grow, but keep the energy and angular momentum indices of $\Phi^{(N)}_{\nu,m}(\rho)$ finite. That is, $n = \frac{1}{2}(N + \nu - |m|) = j + m_y$ and $m = m_x - m_y$ remain finite. As in (109), (110), the integer radii $0 \leqslant \rho \leqslant N$ are to be replaced by a coordinate scaled as $\mathbf{Q}$ in (109). We use Stirling's asymptotic formula for the Γ functions to write

$$r := \rho/\sqrt{j} \in \{0, 1/\sqrt{j}, \ldots, 2\sqrt{j} \to \infty\}, \tag{112}$$

$$\lim_{N\to\infty} \begin{pmatrix} \text{left factor} \\ \text{in (98)} \end{pmatrix} = \sqrt{\frac{2(n+m)!}{n!}}\, r^{m+1/2}, \tag{113}$$

$$\lim_{N\to\infty} {}_3F_2 \left(\begin{matrix} -n,\ -\rho,\ \rho+1 \\ m+1,\ -N \end{matrix} \,\middle|\, 1 \right) = {}_1F_1\left(-n,\, m+1;\, r^2\right) = \\ = \frac{m!\, n!}{(n+m)!} L_n^m(r^2). \tag{114}$$

Thus we obtain the limit of the wavefunctions to be

$$\lim_{N\to\infty} N^{1/4}\,(-1)^N\, \Phi^{(N)}_{\nu,m}(\rho) = \\ = (-1)^n \sqrt{\frac{2\,n!}{(n+m)!}}\, r^{|m|+1/2}\, \mathrm{e}^{-\frac{1}{2}r^2}\, L_n^{|m|}(r^2). \tag{115}$$

The factor $r^{1/2}$ is the square root of the continuum radial integration measure $r\,dr$.

4.12. Contraction of the Schrödinger Equation. We rescale the integer radii ρ to the dimensionless variable r as in (112), keeping the Taylor series of $\exp\,(j^{-1/2}\partial_r)$ to terms of second-order, and divide by r^2. In the limit $N \to \infty$, the difference Eq. (105) becomes the following differential equation:

$$\frac{1}{2}\left[-\frac{d^2}{dr^2} - \frac{1}{r}\frac{d}{dr} + r^2 + \frac{m^2}{r^2}\right]\, \varphi_{n,m}(r) \quad = \quad (2n + m + 1)\, \varphi_{n,m}(r), \tag{116}$$

$$\text{for} \quad \sqrt{r}\, \varphi_{n,m}(r) = \lim_{N\to\infty} \Phi^{(N)}_{\nu,m}(\rho), \tag{117}$$

with $N+\nu = 2n+|m|$, and corresponding to the energies $E = \hbar\omega(2n+|m|+1)$. This is easily recognized as the Schrödinger equation for the two-dimensional radial oscillator of angular momentum m [41].

5. CONCLUSION: DISCRETE AND FINITE FOURIER TRANSFORMS

The original motivation to introduce finite oscillator models was to use their dynamical evolution to define *Fourier-like* transforms between position and momentum representations of discrete and finite, but nonperiodic data sets [5]. Such transforms are the basis for a deeper understanding of the *compact* phase space of finite Hamiltonian systems through their Wigner function.

5.1. Why Not the Ordinary Finite Fourier Transform? The well-known finite Fourier transform $\mathcal{F}$ between $N+1$ «position» values $f = \{f_q\}_{q=0}^N$ and their conjugate «momentum» values $\widetilde{f} = \{\widetilde{f}_p\}_{p=0}^N = \mathcal{F} : f$ is defined by

$$\begin{aligned} \widetilde{f}_p &:= \frac{1}{\sqrt{N+1}} \sum_{q=0}^{N} f_q \, \mathrm{e}^{-2\pi i q p/(N+1)}, \\ f_q &= \frac{1}{\sqrt{N+1}} \sum_{p=0}^{N} \widetilde{f}_p \, \mathrm{e}^{+2\pi i q p/(N+1)}. \end{aligned} \tag{118}$$

It intertwines discrete, finite position space $\Re^{N+1}$ with a similar wavenumber space, where points 0 and N are first neighbors, as for example elongations of a vibrating collection of masses joined by springs [35, Part I], forming a circle of $N+1$ discrete points, $\mathcal{S}^1_{(N+1)}$.

When the position and wavenumber circles are joined in direct product to build a phase space, one obtains a discrete *torus*, $\mathcal{T}^2_{((N+1)^2)} = \mathcal{S}^1_{(N+1)} \otimes \mathcal{S}^1_{(N+1)}$, of $(N+1)^2$ points [13, 14]. There, the finite Fourier transform exchanges the two circles. Now, in contradistinction to the Fourier *integral* transform between $\mathcal{L}^2(\Re)$ Hilbert spaces, which can be fractionalized to rotations of the phase plane $\Re^2$ [3], corresponding to harmonic oscillator evolution, there is *no* continuous group of transformations of the surface of the torus $\mathcal{T}^2$ that will connect the identity to the Fourier transform of exchanged circles. Here we collect the results of [5, 6, 9] that provide proper one-parameter groups of fractional Fourier–Kravchuk and Hankel–Hahn transforms between the data sets of Secs. 3 and 4, respectively.

5.2. Fractional Fourier–Kravchuk Transforms. The time evolution of the finite oscillator is generated by the Hamiltonian H which rotates the Q–P plane. This is an inner automorphism of the $su(2)$ algebra,

$$\mathrm{e}^{-i\phi H} \begin{pmatrix} Q \\ P \end{pmatrix} \mathrm{e}^{i\phi H} = \begin{pmatrix} \cos\phi & \sin\phi \\ -\sin\phi & \cos\phi \end{pmatrix} \begin{pmatrix} Q \\ P \end{pmatrix}. \tag{119}$$

In this context, the *Fourier–Kravchuk* transform $\mathcal{K}$, and its group of fractional powers, acting on $N{+}1$ data points $f = \{f_q\}_{q=0}^{N}$, where the points 0 and N are literally poles apart, is defined in terms of the oscillator evolution by the operator

$$\mathcal{K}^{\alpha} := \exp\left(-i\frac{1}{2}\pi\alpha\left(J_3 + \frac{1}{2}N\right)\right) = \exp\left(+i\frac{1}{4}\pi\alpha\right)\,\exp\left(-i\frac{1}{2}\pi\alpha H\right), \quad (120)$$

where the $su(2)$ generator J_3 and the oscillator Hamiltonian H relate as in (16), and the angle $\phi|_0^{2\pi}$ is replaced by the *power* $\alpha = 2\phi/\pi$ of $\mathcal{K}$. Evidently $\mathcal{K}^{\alpha_1}\,\mathcal{K}^{\alpha_2} = \mathcal{K}^{\alpha_1+\alpha_2}$ and $\mathcal{K}^0 = \hat{1} = \mathcal{K}^4$, so they form an $SO(2)$ group. The «phase correction» by $\dfrac{1}{4}\pi\alpha = \dfrac{1}{2}\phi$ in (120) implies that in both the finite and continuous cases, the fractional Fourier (–Kravchuk) transform multiplies the nth oscillator state by the same phase

$$\mathcal{K}^{\alpha}\Phi_n^{(N)}(q) = \mathrm{e}^{-i\frac{1}{2}\pi n\alpha}\Phi_n^{(N)}(q), \quad n|_0^N. \quad (121)$$

Functions $\Psi^{(N)}(q)$ on the $N{+}1$ points of the discrete position $q|_{-N/2}^{N/2}$ can be arranged as a column vector, on which the Fourier–Kravchuk transform will act through a matrix. This matrix represents $so(3)$ rotations around the 3-axis in the eigenbasis of the 1-axis of positions, and its kernel is given through a Wigner little-d function,

$$\mathcal{K}^{\alpha} : \Psi^{(N)}(q) \mapsto \Psi^{(N,\alpha)}(q) = \sum_{q'=-N/2}^{N/2} K_{q,q'}^{(N,\alpha)}\Psi(q'),\ \Psi^{(N,0)}(q) = \Psi^{(N)}(q), \quad (122)$$

$$K_{q,q'}^{(N,\alpha)} := {}_1\langle N,q|\,\mathrm{e}^{-i\frac{1}{2}\pi\alpha(J_3+j)}\,|N,q'\rangle_1 =$$

$$= \mathrm{e}^{-i\frac{1}{4}\pi N\alpha}\,(-i)^{q-q'}\,d_{q,q'}^{N/2}\left(\frac{1}{2}\pi\alpha\right) = \quad (123)$$

$$= \sum_{n=0}^{N}\Phi_n^{(N)}(q)\,\mathrm{e}^{-i\frac{1}{2}\pi n\alpha}\,\Phi_n^{(N)}(q'), \quad (124)$$

see [18, Eq. 4.7(5)]. The kernel is unitary: $K_{q,q'}^{(N,-\alpha)} = (K_{q',q}^{(N,\alpha)})^*$, and represents the group $SO(2)$ with α modulo 4.

When $N \to \infty$, we expect the Fourier–Kravchuk transform summation kernel (123), (124) to become the Fourier transform integral kernel. To prove this, we use (50) and a particular case of Mehler's formula for Hermite functions $\Psi_n(x)$ [23, 29, 42], namely

$$\sum_{n=0}^{\infty} i^n\Psi_n(x_1)\Psi_n(x_2) = \frac{1}{\sqrt{2\pi}}\,\exp(ix_1x_2). \quad (125)$$

The contraction limit of the kernel (124), when $N = 2j \to \infty$ and $m \to -\infty$ such that $j + m = n$ is fixed and finite, rescaling as before $q = x\sqrt{j}$, $q' = x'\sqrt{j}$, results now in

$$\lim_{N\to\infty} \sqrt{j}\, K^{(N,1)}_{q,q'} = \lim_{N\to\infty} \sqrt{j}\, d^{j}_{q',q}\left(\frac{1}{2}\pi\right) = \frac{1}{\sqrt{2\pi}}\, \mathrm{e}^{ix'x}, \tag{126}$$

namely the Fourier integral transform kernel.

5.3. Fractional Hankel–Hahn Transforms. In two dimensions, the symmetry group of the quantum oscillator is the group of $U(2)$-Fourier transforms [43]. The integral kernel of the $U(1)$ centre of this group can be decomposed into a series Hankel transforms of integer order m, times Fourier series transforms in the angle [35, Ch. 9]. For each angular momentum subspace $\pm m$, the integral transform kernel is a Bessel function $J_m(k^2 r' r)$ in the (continuous) radial coordinate $r|_0^\infty$.

Now, in the two-dimensional finite radial oscillator model, the operator of mode number is $H - 1 = J + E_J$, $E_J = j\hat{1}$, as in (64). As in the one-dimensional case (120), the *fractional Fourier operator* is:

$$\mathcal{F}^\alpha = \exp\left(-i\frac{1}{2}\pi\alpha(J + E_J)\right), \tag{127}$$

of power α modulo 4. In the basis of the mode and angular momentum eigenfunctions of J and M, $\Phi^{(N)}_{\nu,m}$ (see (68)–(71) and (87)–(89)), the Fourier operator (127) is represented by the diagonal matrix

$$F^\alpha_{JM}(\nu, m; \nu', m') = {}_{JM}\langle N; \nu, m|\mathcal{F}^\alpha\, |N; \nu', m'\rangle_{JM} = \\ = \delta_{\nu,\nu'}\, \delta_{m,m'}\, \mathrm{e}^{-i\frac{1}{2}\pi(\nu+j)\alpha}. \tag{128}$$

On the other hand, in the Gel'fand–Tsetlin basis of the radius and angular momentum eigenfunctions of $(\mathbf{R})^2$ and M, $\Phi^{(N)}_{\cdot,m}(\rho)$ (see (78), (79)), the Fourier operator (127) is represented by [42]

$$F^{(N,\alpha)}_R(\rho, m; \rho', m') = {}_R\langle N; \rho, m|\mathcal{F}^\alpha\, |N; \rho', m'\rangle_R = \\ = \delta_{m,m'}\, H^{(N,\alpha)}_m(\rho, \rho'), \tag{129}$$

where, recalling $T(\chi)$ from (83),

$$H^{(N,\alpha)}_m(\rho, \rho') = {}_R\langle N; \rho, m|\mathcal{F}^\alpha\, |N; \rho', m\rangle_R = \tag{130}$$

$$= \sum_{\nu=-N+|m|:(+2)}^{N-|m|} {}_R\langle N; \rho, m|N; \nu, m\rangle_{JM} \times \\ \times\, \mathrm{e}^{-i\frac{1}{2}\pi(\nu+j)\alpha}\, {}_R\langle N; \nu, m|N; \rho', m\rangle_R = \tag{131}$$

$$= \sum_{\nu=-N+|m|:(+2)}^{N-|m|} (-1)^{\rho+\rho'} C^{j,j,\rho}_{\frac{1}{2}(m+\nu),\frac{1}{2}(m-\nu),m} \times$$

$$\times \, \mathrm{e}^{-i\frac{1}{2}\pi(\nu+j)\alpha} C^{j,j,\rho'}_{\frac{1}{2}(m+\nu),\frac{1}{2}(m-\nu),m} = \quad (132)$$

$$= \; {}_{GT}\langle N;\rho,m|T\left(\frac{1}{2}\pi\right)^{-1} \mathrm{e}^{-i\frac{1}{2}\pi\alpha\Lambda_{1,2}} T\left(\frac{1}{2}\pi\right)|N;\rho',m\rangle_{GT} = \quad (133)$$

$$= \; {}_{GT}\langle N;\rho,m|\,\mathrm{e}^{-i\frac{1}{2}\pi\alpha\Lambda_{3,4}}|N;\rho',m\rangle_{GT} =: d^{N,0}_{\rho,m,\rho'}\left(\frac{1}{2}\pi\alpha\right). \quad (134)$$

In the last expression, $d^{N_1,N_2}_{\ell,m,\ell'}(\theta)$ is the $SO(4)$-analogue of the $SO(3)$-Wigner little-d's [44,45], i.e., the matrix elements of the $so(4)$ rotation out of the canonical $so(3)$, in the generic representation (N_1,N_2), where $N_1 \geqslant \ell,\ell' \geqslant |N_2|$ and $\ell,\ell' \geqslant |m|$.

The matrices (129) are block-diagonal in m, because angular momentum M commutes with the generator of the Fourier transform, $J + E_J$. These are $(N-|m|)\times(N-|m|)$ submatrices, with rows and columns numbered by $\rho,\rho' \in \{|m|,|m|+1,\ldots,N\}$. Since the wavefunction basis involves dual Hahn polynomials, we have christened these matrices as *fractional Hankel–Hahn* transforms [9].

The Hankel–Hahn transforms are unitary, finite-N approximations to the Hankel integral transforms. Indeed, we have shown that, for $N\to\infty$, the summation kernel (132) of the former becomes the integral kernel of the latter [40]. Indeed, when $\rho = r\sqrt{N}$ and $\rho' = r'\sqrt{N}$, while radial mode number $n = \nu + j$ and angular momentum m remain finite, the Hankel–Hahn transform matrix kernel contracts to the Hankel transform integral kernel:

$$\lim_{N\to\infty} H^{(N,1)}_m(\rho,\rho') = \quad (135)$$

$$= \sum_{n=0}^{\infty}(-1)^n \frac{2\,n!}{(n+|m|)!}(rr')^{|m|+1/2}\,\mathrm{e}^{-1/2(r^2+r'^2)} L^{|m|}_n(r^2)L^{|m|}_n(r'^2) = \quad (136)$$

$$= i^m\sqrt{rr'}\,J_m(rr'). \quad (137)$$

We note that for $|m|>0$, Hankel–Hahn transforms are defined only on the $N-|m|$ points inside the interval (101), i.e., $|m| \leqslant \rho \leqslant N$. This is the finite counterpart of the ordinary Hankel integral transform kernel $J_m(r'r)$ to have an $|m|$-fold zero at the origin.

5.4. Phase Space for Finite Systems. Hamiltonian systems naturally call for a phase space with coordinates of position and momentum and a Wigner quasiprobability distribution function. In Ref. 15 we introduced such a function

on the $\Re^3$ space of the Lie algebra $su(2)$. In the one-dimensional oscillator case of Sec. 3, the Casimir operator (12) essentially restricts this space to a sphere of radius $\sqrt{j(j+1)}$, which becomes the phase space for a $(2j+1)$-point finite oscillator. Under Hamiltonian evolution this sphere rotates around its J_3 axis, carrying with it that Wigner function; a $\frac{1}{2}\pi$ turn is the Fourier–Kravchuk transform. Under appropriate projections on the position or momentum axes, we can follow the wavefield evolution in the modelled finite oscillator, shallow optical guide, or data set, where the ground state is invariant. From this ground state, through rotations out of the J_3 axis, one can define finite coherent states; these will slightly change their aspect in the cycle though, since they are the parallel projection of the Wigner function on the surface of a rotating sphere. This Wigner function has been shown to reduce [47] to the commonly used Wigner function over a sphere for spin systems [48] and is amenable to be used in nonlinear optical systems [46]. In [49], this Wigner function was generalized to any Lie algebra and related to wavelet transforms.

There are also generalizations of these constructions to other Lie algebras, including $so(2,1)$ for discrete but infinite systems, which involve Meixner polynomials and Bargmann d functions [39, 50, 51], and $iso(2)$ with Bessel functions [52]. Finally, not only Lie algebras but q algebras satisfy the finite oscillator postulates [22], with a nonlinear function f in the basic commutator (8) defining a finite q oscillator. In this case, the «sensor» set of points concentrates towards the centre of the symmetric interval, while the energy spectrum remains equally spaced, and its eigenfunctions are dual q-Kravchuk functions. Since the invariant Casimir operator is now nonquadratic in all generators, the corresponding phase space is not a sphere, but a q-dependent pear-shaped spheroid, tip-up for $q < 1$ and tip-down for $q > 1$. The q-harmonic oscillator evolution (i.e., a phase times the so-defined fractional q-Fourier–Kravchuk transform) will rotate this space around the J_3 symmetry axis of the spheroid. The appropriate definition of a Wigner function is still lacking.

5.5. Unitary Precontraction of Integral Transforms. It has not been satisfactorily explained why the symmetry groups of discrete systems can enlarge in the continuum limit. Some authors [53] have forced the states of a system into multiplets of an extraneous group by writing algebras of «operators» that contain square roots of the Casimir operators, which do not belong to the universal enveloping algebra. Other authors working with finite models, especially those based on the very important Harper functions [32], whose energy spectrum is not equally spaced, import the oscillator periodic motion.

We should stress the convenience of approximating integral transforms by *unitary* matrix kernels on a finite set of points, with the same oscillator dynamics and with guaranteed convergence under contraction. The one-dimensional finite oscillator and its Fourier–Kravchuk transform provides such a precontracted for

the Fourier transform. The two-dimensional model solves the problem of defining unitary, invertible rotations of square pixellated images. Although this problem has been mentioned in the literature [54], it has not been subject to a thorough search outside the standard (and highly refined) numerical methods (in sonar acoustics [55], for example) to evaluate the Hankel transform on a finite polar array. Also, there is a clear avenue to the problem of unitarily transforming pixellated images between Cartesian and polar arrays.

From the point of view of special function theory, the host of known properties of the Wigner $so(3)$ and $so(4)$ little-d and Clebsch–Gordan functions, such as unitarity, parities, bilinear composition, etc., can be used well for finite transforms. Previously, we only knew that eigenfunctions of the Pöschl–Teller potential (used for scattering [56]) were the coupling coefficients of $so(2,1)$ [57]. Finite polynomials of a discrete variable are thus being incorporated to the list of physically important functions, and a tool for image analysis and computation.

Acknowledgements. We thank Alexei Isaev for useful remarks to improve the manuscript. Support by the Dirección General de Asuntos del Personal Académico, Universidad Nacional Autónoma de México (DGAPA–UNAM) by the grant IN102603 *Optica Matemática* is gratefully acknowledged; the figures were provided by Luis Edgar Vicent and Guillermo Krötzsch.

REFERENCES

1. *Wigner E. P.* Do the Equations of Motion Determine the Quantum Mechanical Commutation Relations? // Phys. Rev. 1950. V. 77. P. 711–712.
2. *Arik M., Atakishiyev N. M., Wolf K. B.* Quantum Algebraic Structures Compatible with the Harmonic Oscillator Newton Equation // J. Phys. A. 1999. V. 32. P. L371–L376.
3. *Ozaktas H. M., Zalevsky Z., Alper Kutay M.* The Fractional Fourier Transform. Chichester: John Wiley, 2000.
4. *Atakishiyev N. M., Wolf K. B.* Approximation on a Finite Set of Points through Kravchuk Functions // Rev. Mex. Fís. 1994. V. 40. P. 366–377.
5. *Atakishiyev N. M., Wolf K. B.* Fractional Fourier–Kravchuk Transform // J. Opt. Soc. Am. A. 1997. V. 14. P. 1467–1477.
6. *Atakishiyev N. M., Vicent L. E., Wolf K. B.* Continuous vs. Discrete Fractional Fourier Transforms // J. Comp. Appl. Math. 1999. V. 107. P. 73–95.
7. *Moshinksy M., Smirnov Yu. F.* The Harmonic Oscillator in Modern Physics. Amsterdam: Hardwood Academic Publishers, 1996.
8. *Atakishiyev N. M., Pogosyan G. S., Vicent L. E., Wolf K. B.* Finite Two-Dimensionsal Oscillator. I. The Cartesian Model // J. Phys. A. 2001. V. 34. P. 9381–9398.
9. *Atakishiyev N. M., Pogosyan G. S., Vicent L. E., Wolf K. B.* Finite Two-Dimensionsal Oscillator. II. The Radial Model // Ibid. P. 9399–9415.
10. *Miller W. Jr.* Symmetry Groups and Separation of Variables // Encyclopedia of Mathematics. Addison-Wesley, Reading, 1977. V. 4.

11. *Santhanam T. S., Tekumalla A. R.* Quantum Mechanics in Finite Dimensions // Found. Phys. 1976. V. 6. P. 583–589;
Mehta M. L. Eigenvalues and Eigenvectors of the Finite Fourier Transform // J. Math. Phys. 1987. V. 28. P. 781–785;
Santhanam T. S. Finite-Space Quantum Mechanics and Krawtchuk Functions // Proc. of the Workshop on Special Functions and Differential Equations. Delhi, 1998.

12. *Belingeri C., Ricci P. E.* A Generalization of the Discrete Fourier Transform // Int. Transf. Spec. Funct. 1995. V. 3. P. 165–174.

13. See, e.g. *Pei S.-C., Yeh M.-H.* Improved Discrete Fractional Transform // Opt. Lett. 1997. V. 22. P. 1047–1049;
Richman M. S., Parks T. W., Shenoy R. G. Discrete-Time, Discrete-Frequency Analysis // IEEE Trans. Signal Proc. 1998. V. 46. P. 1517–1527.

14. *Hakioğlu T.* Fenite-Dimensional Schwinger Basis. Deformed Symmetries, Wigner Function, and an Algebraic Approach to Quantum Phase. // J. Phys. A. 1998. V. 31. P. 6975;
Hakioğlu T. Linear Canonical Transformations and Quantum Phase: a Unified Canonical and Algebraic Approach. // J. Phys. A. 1999. V. 32. P. 4111;
*Hakioğlu T.*Operational Approach in the Weak-Field Measurement of Polarization Fluctuations // Phys. Rev. A. 1999. V. 59. P. 1586;
Hakioğlu T., Wolf K. B. The Canonical Kravchuk Basis for Discrete Quantum Mechanics // J. Phys. A. 2000. V. 33. P. 3313–3323.

15. *Atakishiyev N. M., Chumakov S. M., Wolf K. B.* Wigner Distribution Function for Finite Systems // J. Math. Phys. 1998. V. 39. P. 6247–6261.

16. *Ali S. T., Atakishiyev N. M., Chumakov S. M., Wolf K. B.* The Wigner Function for General Lie Groups and the Wavelet Transform // Ann. H. Poincaré. 2000. V. 1. P. 685–714.

17. *Wolf K. B.* Dynamical Groups for the Point Rotor and the Hydrogen Atom // Supp. Nuovo Cim. 1967. V. 5. P. 1041–1050.

18. *Varshalovich D. A., Moskalev A. N., Khersonskiĭ V. K.* Quantum Theory of Angular Momentum. Singapore: World Scientific, 1988.

19. *Krawtchouk M.* Sur une Généralization des Polinômes d'Hermite // C. R. Acad. Sci. Paris. 1929. V. 189. P. 620–622.

20. *Atakishiyev N. M., Suslov S. K.* Difference Analogs of the Harmonic Oscillator // Theor. Math. Phys. 1991. V. 85. P. 1055–1062.

21. *Vilenkin N. Ja., Klimyk A. U.* Representation of Lie Groups and Special Functions. Dordrecht, 1991. V. 1. P. 346.

22. *Atakishiyev N. M., Klimyk A. U., Wolf K. B.* Finite q-Oscillator // J. Phys. A. 2004. V. 37. P. 5569–5587.

23. *Atakishiyev N. M., Pogosyan G. S., Vicent L. E., Wolf K. B.* Contraction of the Finite One-Dimensional Oscillator // Intern. J. Mod. Phys. A. 2003. V. 18(2). P. 317–327.

24. *Talman J. D.* Special Functions — a Group Theoretic Approach. N. Y., 1968. Ch. 13.

25. *Arecchi F. T. et al.* Atomic Coherent State in Quantum Optics // Phys. Rev. A. 1972. V. 6. P. 2211–2237.

26. *Gilmore R.* Lie Groups, Lie Algebras, and Some of Their Applications. N. Y.: John Wiley & Sons, 1974.

27. *Pogosyan G. S., Sissakian A. N., Winternitz P.* Separation of Variables and Lie Algebra Contractions. Applications to Special Functions // Part. Nucl. 2002. V. 33, Suppl. 1. P. S1123–S1144.

28. *Izmest'ev A. A., Pogosyan G. S., Sissakian A. N., Winternitz P.* Contractions of Lie Algebras and the Separation of Variables. Interbasis Expansions // J. Phys. A. 2001. V. 34. P. 521–554.

29. *Erdélyi A., Magnus W., Oberhettinger F., Tricomi F. G.* Higher Transcendental Functions. N. Y.: McGraw-Hill, 1953. V. 2.

30. *Pogosyan G. S., Ter-Antonyan V. M.* The Connection between Cartesian and Polar Wavefunctions of a Circular Oscillator and the Dynamical $O(3)$ Symmetry // Izv. A. N. Arm. SSR. Fizika. 1978. V. 13. P. 235–237;
Pogosyan G. S., Smorodinsky Ya. A., Ter-Antonyan V. M. Oscillator Wigner functions // J. Phys. A. 1981. V. 14. P. 769–776;
Mardoyan L. A., Pogosyan G. S., Sissakian A. N., Ter-Antonyan V. M. Interbasis Expansions in a Circular Oscillator // Nuovo Cim. A. 1985. V. 86. P. 324–336.

31. *Frank A., Van Isacker P.* Algebraic Methods in Molecular and Nuclear Structure Physics. N. Y., 1998.

32. *Barker L., Çandan Ç., Hakioğlu T., Kutay A., Ozaktas H. M.* The Discrete Harmonic Oscillator, Harper's Equation, and the Discrete Fractional Fourier Transform // J. Phys. A. 2000. V. 33. P. 2209–2222.

33. *Stone A. P.* Some Properties of Wigner Coefficients and Hyperspherical Harmonics // Proc. Camb. Phil. Soc. 1956. V. 52. P. 424–430.

34. *Biedenharn L. C., Louck J. D.* Angular Momentum in Quantum Physics // Encyclopedia of Mathematics and Its Applications. Addison-Wesley, Reading, 1981.

35. *Wolf K. B.* Integral Transforms in Science and Engineering. N. Y.: Plenum Publ. Corp., 1979.

36. *Hahn W.* Über Orthogonalpolynome, die q-Differenzengleichungen Genügen // Math. Nachr. 1949. V. 2. P. 4–34.

37. *Nikiforov A. F., Suslov S. K., Uvarov V. B.* Classical Orthogonal Polynomials of a Discrete Variable // Springer Series in Comp. Phys. Heidelberg, 1991. Eqs. (5.2.13), (5.2.14).

38. *Koekoek R., Swarttow R. F.* The Askey-Scheme of Hypergeometric Orthogonal Polynomials and its q-Analogue. Report No. 98-17. Delft, 1998. P. 34.

39. *Atakishiyev N. M., Nagiyev Sh. M., Vicent L. E., Wolf K. B.* Covariant Discretization of Axis-Symmetric Linear Optical Systems // J. Opt. Soc. Am. A. 2000. V. 17. P. 2301–2314.

40. *Atakishiyev N. M., Pogosyan G. S., Wolf K. B.* Contraction of the Finite Radial Oscillator // Intern. J. Mod. Phys. A. 2003. V. 18(2). P. 329–341.

41. *Flügge S.* Practical Quantum Mechanics. 2nd ed. Berlin, 1994. P. 107–110.

42. *Namias V.* Fractionalization of Hankel Transforms // J. Inst. Maths. Appl. 1980. V. 26. P. 187–197.

43. *Simon R., Wolf K. B.* The Structure of Paraxial Optical Systems // J. Opt. Soc. Am. A. 2000. V. 17. P. 342–355;
Simon R., Wolf K. B. Fractional Fourier Transforms in Two Dimensions // Ibid. P. 2368–2381.

44. *Biedenharn L. C.* Wigner Coefficients for the R_4 Group and Some Applications // J. Math. Phys. 1961. V. 2. P. 433–441;
Freedman D. Z., Wang J.-M. $O(4)$ Symmetry and Regge-Pole Theory // Phys. Rev. 1967. V. 160. P. 1560–1571.

45. *Wolf K. B.* A Recursive Method for the Calculation of the SO_n, $SO_{n,1}$, and ISO_n Representation Matrices // J. Math. Phys. 1971. V. 12. P. 197–206.

46. *Chumakov S. M., Frank A., Wolf K. B.* Finite Kerr Medium: Macroscopic Quantum Superposition States and Wigner Functions on the Sphere // Phys. Rev. A. 1999. V. 60. P. 1817–1823.

47. *Chumakov S. M., Klimov A. B., Wolf K. B.* On the Connection of Two Wigner Functions for Spin Systems // Phys. Rev. A. 2000. V. 61. P. 034101(3).

48. *Agarwal G. S.* Relation between Atomic Coherent-State Representation, State Multipoles, and Generalized Phase-Space Distributions // Phys. Rev. A. 1981. V. 24. P. 2889;
see also *Stratonovich R. L.* // Sov. Phys. JETP. 1956. V. 31. P. 1012;
Dowling J. P., Agarwal G. S., Schleich W. P. Wigner Distribution of a General Angular-Momentum State: Applications to a Collection of Two-Level Atoms // Phys. Rev. A. 1994. V. 49. P. 4101;
Agarwal G. S., Puri R. R.-, Singh R. P. Atomic Schrödinger Cat States // Phys. Rev. A. 1997. V. 56. P. 2249.

49. *Ali S. T., Atakishiyev N. M., Chumakov S. M., Wolf K. B.* The Wigner Function for General Lie Groups and the Wavelet Transform // Ann. H. Poincaré. 2000. V. 1. P. 685–714.

50. *Bargmann V.* Unitary Irreducible Representations of the Lorentz Group // Ann. Math. 1947. V. 48. P. 568–640.

51. *Atakishiyev N. M., Jafarov E. I., Nagiyev Sh. M., Wolf K. B.* Meixner Oscillators // Rev. Mex. Fís. 1998. V. 44. P. 235–244.

52. *Nieto L. M., Atakishiyev N. M., Chumakov S. M., Wolf K. B.* Wigner Distribution Function for Euclidean Systems // J. Phys. A. 1998. V. 31. P. 3875–3895.

53. *Moshinsky M., Seligman T. H.* Canonical Transformations to Action and Angle Variables and Their Representation in Quantum Mechanics // Ann. Phys. (N. Y.). 1978. V. 114. P. 243–259; II. The Coulomb Problem // Ann. Phys. (N.Y.). 1979. V. 120. P. 430–445; III. The General Problem (with Deenen J.) // Ann. Phys. (N. Y.). 1980. V. 127. P. 458–466.

54. *Richman M. S., Parks T. W., Shenoy R. G.* Discrete-Time, Discrete-Frequency Analysis // IEEE Trans. Signal Proc. 1998. V. 46. P. 1517–1527.

55. *Candel S. M.* An Algorithm for the Fourier–Bessel Transform // Comp. Phys. Commun. 1981. V. 23. P. 343;
Secada J. D. Numerical Evaluation of the Hankel Transform // Comp. Phys. Commun. 1999. V. 116. P. 278–294.

56. *Frank A., Wolf K. B.* Lie Algebras for Potential Scattering // Phys. Rev. Lett. 1984. V. 52. P. 1737–1739;
Frank A., Wolf K. B. Lie Algebras for Systems with Mixed Spectra. The Scattering Pöschl–Teller Potential // J. Math. Phys. 1985. V. 26. P. 973–985.

57. *Basu D., Wolf K. B.* The Clebsch–Gordan Coefficients of the Three-Dimensional Lorentz Algebra in the Parabolic Basis // J. Math. Phys. 1983. V. 24. P. 478–500.